

# NORSAR

ROYAL NORWEGIAN COUNCIL FOR SCIENTIFIC AND INDUSTRIAL RESEARCH

12 JK

ADA 033848

Scientific Report No. 1-76/77

## FINAL REPORT NORSAR PHASE 3

1 July - 30 September 1976

Prepared by  
K.-A. Berteussen

DDC  
RECEIVED  
DEC 20 1976  
C

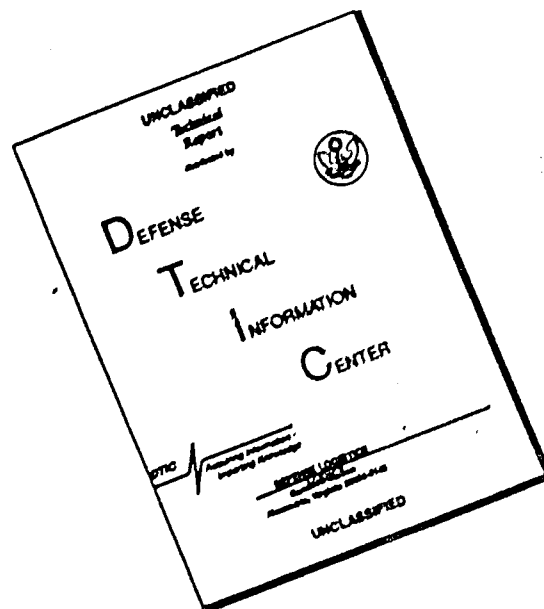
Kjeller, 27 October 1976

Sponsored by  
Advanced Research Projects Agency  
ARPA Order No. 2551



APPROVED FOR PUBLIC RELEASE, DISTRIBUTION UNLIMITED

# DISCLAIMER NOTICE



THIS DOCUMENT IS BEST QUALITY AVAILABLE. THE COPY FURNISHED TO DTIC CONTAINED A SIGNIFICANT NUMBER OF PAGES WHICH DO NOT REPRODUCE LEGIBLY.

REPORT DOCUMENTATION PAGE		READ INSTRUCTIONS BEFORE COMPLETING FORM
1. REPORT NUMBER F08606-76-C-0001	2. GOVT ACCESSION NO.	3. RECIPIENT'S CATALOG NUMBER
4. TITLE (and Subtitle) FINAL REPORT - NORSAR PHASE 3 The Norwegian Seismic Array (NORSAR) Phase 3.	5. TYPE OF REPORT & PERIOD COVERED FINAL REPORT. 1 Jul - 30 September 1976	6. PERFORMING ORG. REPORT NUMBER Sci. Rep. No. 1-76/77
7. AUTHOR(s) K.-A. Berteussen (Editor)	8. CONTRACT OR GRANT NUMBER(s) F08606-76-C-0001 ✓ ARPA Order-2551	9. PERFORMING ORGANIZATION NAME AND ADDRESS NTNF/NORSAR Post Box 51 2007 Kjeller, Norway
10. CONTROLLING OFFICE NAME AND ADDRESS	11. REPORT DATE 27 October 1976	12. NUMBER OF PAGES 71
13. MONITORING AGENCY NAME & ADDRESS (if different from Controlling Office) VELA Seismological Center 314 Montgomery Street Alexandria, Va. 22314	14. SECURITY CLASS. (of this report)	15a. DECLASSIFICATION/DOWNGRADING SCHEDULE
16. DISTRIBUTION STATEMENT (of this Report)  APPROVED FOR PUBLIC RELEASE, DISTRIBUTION UNLIMITED.		
17. DISTRIBUTION STATEMENT (of the abstract entered in Block 20, if different from Report)  NORSAR - Scientific - 1-76/77		
18. SUPPLEMENTARY NOTES		
19. KEY WORDS (Continue on reverse side if necessary and identify by block number)		
20. ABSTRACT (Continue on reverse side if necessary and identify by block number)  This report covers research and operations activities at the Norwegian Seismic Array (NORSAR) for the period 1 July -30 September 1976. This is the last period where the full (22 subarray) array configuration is retained.  Within the reporting period there have been 170 breaks in the otherwise continuous operation of the Detection Processor (DP). The uptime percentage is 96.6. Three operators left in the period, and the vacant positions		

407 283

were covered by substitutes and overtime by the other operators. The bulletin production under the full-sized NORSAR has now been discontinued and some statistics for the period 1971-1976 are given. Altogether about 70 000 processings have been completed by the Event Processor (EP) out of which approximately 36 000 have been accepted as true events. In the DP a number of modifications have been performed in order to adapt the system to an environment with only 7 subarrays. At subarray 01B it has been technically checked out that in the new array configuration it will be possible to send attenuated long period (LP) data in parallel to the ordinary data flow. The performance of the array instrumentation has been satisfactory. Five reports/papers have been finished and four topics are covered in the summary of research activities. It has previously been reported on a project where 2.778 Hz monochromatic waves from a hydroelectric power plant have been used for precise monitoring of seismic velocities. A three-component short period seismometer set has been installed in site 14C02, and using data from these instruments it is demonstrated that the waves have an S-type particle motion. In the weighted beamforming process previously studied at NORSAR, also negative amplitude weights were allowed. This occasionally led to undesirable side effects, and in the second study reported herein it is described how this problem may be avoided. In the third study simulated data is used in order to find out what sort of information one may obtain about the crust by using spectra of long period P-waves. Finally is reported on a study of the variance of teleseismic P-wave amplitudes, where it is indicated that world-wide  $m_b$  scatter increases with decreasing magnitude, and that magnitude bias studies based on large events will not necessarily be adequate at low magnitudes.

Three appendices are included in this report. Appendix A describes the format of the NORSAR High Rate tape while Appendix B describes the format of the Low Rate tape for data after 1 October 1976. In Appendix C the new array beam deployment is described.

ACCESSION for

NTIS

DOC

UNANNOUNCED

DISTRIBUTION

BY

DIST. BY

DATE

A

AFTAC Project Authorization No. : VT/6702/B/ETR

ARPA Order No. : 2551, Amendment 8

Program Code No. : 6F10

Name of Contractor : Royal Norwegian Council for Scientific  
and Industrial Research

Effective Date of Contract : 1 July 1975

Contract Expiration Date : 30 September 1976

Contract No. : F08606-76-C-0001

Project Manager : Nils Marås (02) 71 69 15

Title of Work : The Norwegian Seismic Array (NORSAR)  
Phase 3

Amount of Contract : \$1 000 134

Contract Period Covered by the  
Report : 1 July 1976 - 30 September 1976

The views and conclusions contained in this document are those of the authors and should not be interpreted as necessarily representing the official policies, either expressed or implied, of the Advanced Research Projects Agency, the Air Force Technical Applications Center, or the U.S. Government.

This research was supported by the Advanced Research Projects Agency of the Department of Defense and was monitored by AFTAC/VSC, Alexandria, Virginia 22313, under contract no. F08606-76-C-0001.

TABLE OF CONTENTS

	<u>Page</u>
I. SUMMARY	1
II. OPERATION OF ALL SYSTEMS	3
II.1 Detection Processor Operation (DP)	3
II.2 Event Processor Operation (EP)	11
II.3 NORSAR Data Processing Center (NDPC) Operation	11
II.4 ARPANET	14
III. ARRAY PERFORMANCE	15
IV. IMPROVEMENTS AND MODIFICATIONS	19
IV.1 Detection Processor	19
IV.2 Event Processor	21
IV.3 Array Instrumentation	22
V. MAINTENANCE ACTIVITY	23
VI. DOCUMENTATION DEVELOPED	28
VI.1 Reports, Papers	28
VI.2 Program Documentation	28
VII. SUMMARY OF SPECIAL TECHNICAL REPORTS/PAPERS PREPARED	29
VII.1 Seismic Velocity Variations and Solid Earth Tides	29
VII.2 Weighted Beamforming using Non-negative Weights	33
VII.3 Long Period P-Wave Spectra as a Tool for Studies of Local Structure	35
VII.4 Variance of Teleseismic P-Wave Amplitudes	42
APPENDIX A - Format of the NORSAR High Rate Data Tape effective 1 October 1976	49
APPENDIX B - Format of the NORSAR Low Rate Data Tape effective 1 October 1976	57
APPENDIX C - NORSAR Array Beam Deployment effective 1 October 1976	65

I. SUMMARY

This report covers research and operations activities at the Norwegian Seismic Array (NORSAR) for the period 1 July - 30 September 1976. This is the last period where the full (22 subarray) array configuration is retained.

Within the reporting period there have been 170 breaks in the otherwise continuous operation of the Detection Processor (DP). The uptime percentage is 96.6. Three operators left in the period, and the vacant positions were covered by substitutes and overtime by the other operators. The bulletin production under the full-sized NORSAR has now been discontinued and some statistics for the period 1971-1976 are given. Altogether about 70 000 processings have been completed by the Event Processor (EP) out of which approximately 36 000 have been accepted as true events. In the DP a number of modifications have been performed in order to adapt the system to an environment with only 7 subarrays. At subarray 01B it has been technically checked out that in the new array configuration it will be possible to send attenuated long period (LP) data in parallel to the ordinary data flow. The performance of the array instrumentation has been satisfactory. Five reports/papers have been finished and four topics are covered in the summary of research activities. It has previously been reported on a project where 2.778 Hz monochromatic waves from a hydroelectric power plant have been used for precise monitoring of seismic velocities. A three-component short period seismometer set has been installed in site 14C02, and using data from these instruments it is demonstrated that the waves have an S-type particle motion. In the weighted beamforming process previously studied at NORSAR, also negative amplitude weights were allowed. This occasionally led to undesirable side effects, and in the second study reported herein it is described how this problem may be avoided. In the third study simulated data is used in order to find out what sort of information

one may obtain about the crust by using spectra of long period P-waves. Finally is reported on a study of the variance of teleseismic P-wave amplitudes, where it is indicated that world-wide  $m_b$  scatter increases with decreasing magnitude, and that magnitude bias studies based on large events will not necessarily be adequate at low magnitudes.

Three appendices are included in this report. Appendix A describes the format of the NORSAR High Rate tape while Appendix B describes the format of the Low Rate tape for data after 1 October 1976. In Appendix C the new array beam deployment is described.

K.-A. Berteussen

II. OPERATION OF ALL SYSTEMS

II.1 Detection Processor Operation

Within the reporting period there have been 170 breaks in the otherwise continuous operation of the Detection Processor (DP) system. The uptime percentage is 96.6%, as compared to 93.8% for the last reporting period (January-July 1976).

Fig. II.1 and the accompanying Table II.1.1 both show the daily DP downtime, in hours, for the days between 1 July and 30 September 1976. The monthly recording times and up percentages are given in Table II.1.2.

The most significant break in the recording occurred on 12 September, when the SPS core memory was overheated and failed. This caused a break of more than 8 hours. A power failure on 9 August caused a stoppage of about 3 hours.

The 170 breaks occurring within the reporting period may be grouped in the following categories:

a) Error on the multiplexor channel	:	67
b) Software related stops	:	41
c) SPS malfunctioning	:	17
d) Tests	:	12
e) EOC unit problems	:	8
f) Tape drive "	:	5
g) TIP related stops	:	5
h) Customs Engineering maintenance	:	4
i) Operation	:	4
j) Unknown reason	:	4
k) Other hardware (TOD, punch)	:	2
l) Power failure	:	1

The unrecoverable error on the multiplexor channel (category a), which was described in the report for the last period, still causes the most frequent breaks. So far no solution has been found to this problem, which is related to the presence of the TIP interface unit on this channel. However, tests performed show that the problem may be circumvented by writing the printer output to a magnetic tape.

As can be seen from Table II.1.1. the software related stops occurred frequently in the beginning of the reporting period, to disappear towards the end of the period. This is related to an internal priority problem of the NCP task, which finally was solved (see under Improvements and Modifications, Chapter IV).

The number of SPS related stops is relatively normal. Category d) shows the number of times the system was taken down to perform some kind of test (i.e., a new version, EOC hardware fix, etc.). The somewhat large number of tests was caused by the discovery that the Secondary Online system could no more be used simultaneously with the Primary Online system, since initialization of the former invariably brought down the SPS. As can be seen from both tables (II.1.1 and II.1.2), the overall situation was improved towards the end of the reporting period, when software related stops were eliminated. The total down time for this period was 75 hours 39 minutes. The mean-time-between-failures was 0.5 days as compared with 0.4 days with the last reporting period (January-July 1976).

D. Rieber-Mohn

TABLE II.1.1

LIST OF BREAKS IN DP PROCESSING THE LAST 3 MONTHS

DAY	START	STOP	COMMENTS.....
183	12	36	12 39 PROGRAM HANGUP,RESTART
183	20	21	20 37 MPX/LATE ERROR
183	22	43	22 50 MPX/LATE ERROR
184	14	55	15 7 EOC RELATED PROG. CHECK
184	15	10	18 10 MPX/LATE,SPS HARDWARE
185	1	33	1 45 PROGRAM ERROR
185	10	42	10 48 EOC PROBLEMS
185	11	23	11 28 EOC PROBLEMS
185	12	40	13 13 MPX/LATE ERROR
186	9	15	9 29 MPX/LATE ERROR
186	15	15	15 42 MPX/LATE ERROR
187	11	20	11 27 SPS SYS HALT
189	6	44	7 10 TAPE DRIVE PROBLEM
189	8	4	8 17 MPX/LATE ERROR
190	8	26	8 31 PROGRAM ERROR
190	11	54	12 0 CHNG OP. DISK PACKS
190	14	20	14 24 PROGRAM HANGUP
191	7	47	7 56 NCP TASK HANGUP
191	11	19	11 22 NCP TASK HANGUP
191	17	14	17 17 PROGRAM CHANGE
191	18	59	19 4 NCP TASK HANGUP
192	13	26	13 34 NCP TASK HANGUP
192	13	50	14 11 TAPE PROBLEMS
192	17	30	17 53 MPX/LATE ERROR
192	18	58	19 12 MPX/LATE ERROR
193	3	5	3 21 REQUESTED FROM CCP
193	3	50	3 55 TIP PROBLEM
193	10	47	10 52 NO TP START TIMES
193	20	32	20 43 TAPE PROBLEMS
194	5	52	6 6 SPS INTER. NOT REC.
195	0	12	0 29 SPS
195	10	3	10 6 PROGRAM HANGUP
195	12	19	12 29 PROGRAM HANGUP
195	20	42	21 13 MPX/LATE ERROR
197	11	37	13 5 EOC MAINT AND REP.
197	13	58	14 15 CPU DISABLED
198	3	44	4 5 MPX/LATE ERROR
198	8	20	8 43 PROGRAM HANGUP
198	22	5	22 54 MPX/LATE ERROR
199	1	45	2 0 CPU DISABLED
199	14	54	15 3 TIP CRASH
201	14	15	14 30 MPX/LATE ERROR
201	23	58	24 0 TIP CRASH
202	0	0	0 38 TIP CRASH
202	1	32	1 39 TIP CRASH
202	11	48	11 54 PROGRAM HANGUP
203	0	18	0 37 MPX/LATE ERROR
203	10	8	10 53 CPU DISABLED
203	22	25	22 36 PROGRAM HANGUP
204	9	20	10 3 UNKNOWN REASON
204	10	50	11 9 CPU DISABLED
204	13	26	13 54 AM TEST

TABLE II.1.1

205	2	17	2	36	MPX/LATE ERROR
205	15	26	15	33	PROGRAM HANGUP
205	17	51	17	58	PROGRAM HANGUP
206	7	24	7	57	MPX/LATE ERROR
206	12	27	12	42	CPU DISABLED
207	8	42	8	59	PROGRAM HANGUP
208	8	49	9	5	AM TEST
209	2	35	2	44	PROGRAM HANGUP
209	21	31	21	35	PROGRAM HANGUP
209	22	25	22	37	MPX/LATE ERROR
210	9	58	10	11	MPX/LATE ERROR
210	18	9	18	17	PROGRAM HANGUP
211	1	16	1	31	MPX/LATE ERROR
211	3	47	3	57	CPU DISABLED
211	4	4	4	28	MPX/LATE ERROR
211	5	20	5	35	MPX/LATE ERROR
211	10	38	10	45	PROGRAM HANGUP
211	21	54	21	58	PROGRAM HANGUP
212	2	0	2	15	MPX/LATE ERROR
212	3	27	3	36	TAPE DRIVE PROBLEMS
212	4	0	4	10	PROGRAM HANGUP
212	12	50	13	0	C. E. 2311
212	20	20	20	34	MPX/LATE ERROR
213	14	45	15	5	UNKNOWN REASON
214	1	6	1	10	PROGRAM HANGUP
214	16	20	16	47	MPX/LATE ERROR
215	13	36	13	57	MPX/LATE ERROR
216	7	23	7	47	PROGRAM CHECK
216	19	17	20	0	C. E. ON A 2311
217	0	3	0	13	PROGRAM HANGUP
217	12	24	12	41	CHANGE OF DISK PACK
217	12	58	13	9	EOC RELATED STOP
218	0	15	0	50	EOC RELATED STOP
218	9	21	9	28	PROGRAM HANGUP
218	11	23	11	51	MPX/LATE ERROR
218	12	11	12	25	MPX/LATE ERROR
219	7	49	8	9	PROGRAM HANGUP
219	9	50	10	19	CE ON 1052
219	14	1	14	13	CHANGE OF DISK PACK
220	1	23	1	28	PROGRAM HANGUP
220	11	45	11	54	PROGRAM HANGUP
221	8	12	8	25	TAPE DRIVE PROBLEMS
221	9	48	10	2	MPX/LATE ERROR
221	16	35	16	46	UNKNOWN REASON
221	18	5	18	20	MPX/LATE ERROR
222	9	15	9	46	MPX/LATE ERROR
222	11	59	14	37	POWER FAILURE
223	13	52	14	10	SPS FAILURE
223	21	18	21	28	PROGRAM HANGUP
224	0	2	0	9	PROGRAM HANGUP
224	10	2	10	20	PROGRAM CHANGE
224	14	24	14	40	MPX/LATE ERROR
224	16	0	16	40	MPX/LATE ERROR

TABLE II.1.1

227	2	3	2	18	MPX/LATE ERROR
229	7	3	7	24	SPS FAILURE
229	14	18	14	28	SPS FAILURE
230	4	33	5	16	MPX/LATE ERROR
230	5	20	5	28	PROGRAM FAILURE
230	23	39	23	54	SPS FAILURE
232	6	19	6	51	MPX/LATE ERROR
232	13	0	13	5	SPS FAILURE
232	17	4	17	25	MPX/LATE ERROR
232	22	41	22	58	MPX/LATE ERROR
233	1	9	1	24	SPS FAILURE
233	1	50	2	11	SPS FAILURE
233	9	27	11	24	SPS ROS TAPE CHANGE
234	13	50	14	8	MPX/LATE ERROR
235	1	37	1	54	MPX/LATE ERROR
236	10	38	10	50	MPX/LATE ERROR
236	13	11	13	28	CE ON 1052
236	22	47	23	2	MPX/LATE ERROR
237	10	13	10	25	EOC MAINTENANCE
238	23	51	24	0	MPX/LATE ERROR
239	0	0	0	2	MPX/LATE ERROR
239	23	58	24	0	MPX/LATE ERROR
240	0	0	0	16	MPX/LATE ERROR
240	7	28	7	48	TEST EOC
241	3	20	3	56	MPX/LATE ERROR
242	11	16	11	42	MPX/LATE ERROR
243	3	58	4	10	MPX/LATE ERROR
243	14	15	14	23	SPS FAILURE
243	16	53	17	6	MPX/LATE ERROR
243	23	39	24	0	MPX/LATE ERROR
244	0	0	0	38	MPX/LATE ERROR
244	15	41	15	51	MPX/LATE ERROR
245	17	40	17	58	UNKNOWN REASON
246	17	35	18	0	MPX/LATE ERROR
249	2	12	2	25	PUNCH FAILURE
249	21	22	21	34	MPX/LATE ERROR
252	7	52	8	17	MPX/LATE ERROR
252	21	42	21	46	TOD FAILURE
253	1	25	1	30	SPS FAILURE
255	15	50	16	6	MPX/LATE ERROR
256	6	24	7	22	MPX/LATE ERROR
256	15	0	22	19	SPS CORE OVERHEATED
257	9	6	9	22	MPX/LATE ERROR
257	17	40	18	25	MPX/LATE ERROR
258	3	15	4	31	MPX/LATE ERROR ETC.
259	13	16	13	34	SPS FAILURE
260	13	51	14	32	SPS FAILURE

TABLE II.1.1

260	22	2	22	8	SPS FAILURE
261	14	6	15	40	TEST NEW VERSION
263	13	30	14	34	MPX/LATE ERROR
264	12	16	13	42	TEST NEW VERSION
265	18	5	18	21	MPX/LATE ERROR
265	20	7	20	32	MPX/LATE ERROR
266	13	40	14	5	TEST NEW VERSION
266	15	38	16	0	MPX/LATE ERROR
266	21	28	22	3	MPX/LATE ERROR
267	12	9	12	20	MPX/LATE ERROR
268	9	51	10	34	TEST NEW VERSION
268	11	55	13	11	TEST NEW VERSION
268	23	54	24	0	MPX/LATE ERROR
269	0	0	0	27	MPX/LATE ERROR
269	7	45	8	31	MPX/LATE ERROR
270	7	23	8	23	MPX/LATE ERROR
270	13	27	13	31	TAKEN DOWN BY OPERATOR
271	8	14	9	3	TEST NEW VERSION
271	12	52	13	34	TEST NEW VERSION
271	18	14	18	46	MPX/LATE ERROR
272	9	11	10	47	TEST NEW VERSION
273	8	1	10	57	TEST NEW VERSION
274	11	34	12	9	START NEW VERSION

TABLE II.1.1.2  
DP and EP computer usage July-September 1976

Month	DP Uptime (HRS)	DP Uptime (%)	No. of DP Breaks	No. of Days with DP Breaks	DP MTBF* (Days)	EP Uptime (HRS)	EP Uptime (%)
Jul	721.4	97.0	75	28	0.4	185.3	24.9
Aug	722.0	97.0	58	27	0.5	192.0	25.8
Sep	689.3	95.8	37	24	0.8	165.0	22.9
Total	2132.7	96.6	170	79	0.5	542.3	24.6

\* Mean-time-between-failures.

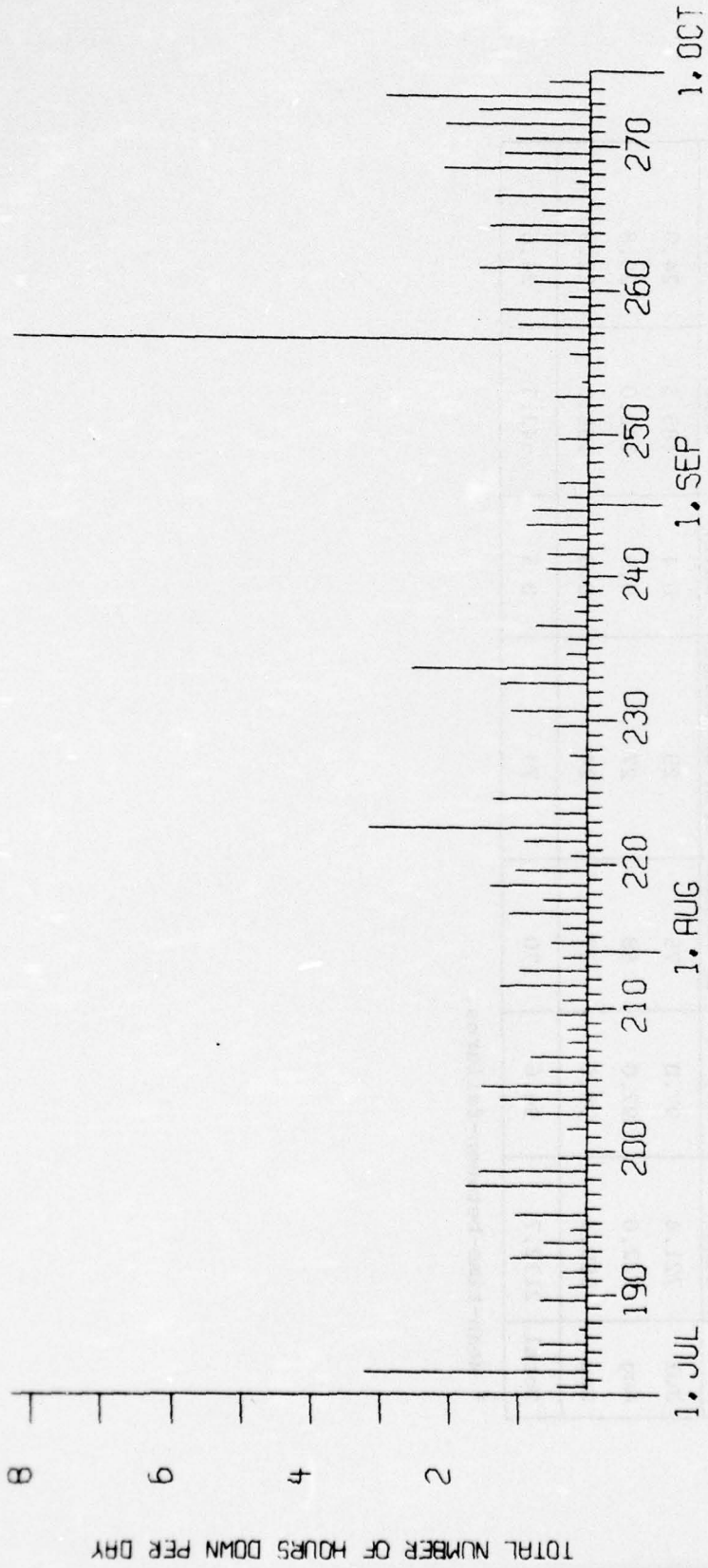


Fig. II.1.1.1 Detection Processor Down Time Jul-Sep 1976.

## II.2 Event Processor Operation (EP)

The Event Processor system has performed satisfactorily throughout the reporting period. Its up time percentage is 24.3, as compared to 29.6 for the last reporting period (January-June 1976).

H. Bungum

## II.3 NORSAR Data Processing Center (NDPC) Operation

### Data Center

The data center operation has been affected by the planned change to unmanned operation. Three operators left in the period. The vacant positions were covered by substitutes and overtime by the other operators.

The Detection Processor up time was 96.6% for the period. Here bugs in and testing of the new DP version stand for about 1% of the down time.

The SPS had two major stops, both times it was put back into operation by project personnel. Also on the EOC project personnel have been engaged in fault-finding maintenance.

The power situation was fairly good; thunderstorms usually cause a number of power breaks in this period.

### Data Communication

The Terminal Interface Message Processor (TIP)

After a power outage 9 August the TIP could not be restarted and Mr. Kelly (Bolt, Beranek and Newman) had to be called in from London. After this incident the TIP has performed as normal. The power supply was replaced 23 August. Further corrections to the TIP have not been made since the last report.

National Communication Circuits

Outages have occurred sporadically and groups of subarrays have been affected. Individual subarrays have also been subject to outages or deteriorated performance due to:

- Cable faults (06B)
- Line trouble/EPU power interference (01C)
- Broken cable (02C)
- NTA-work (PCM-installation in the area) (02B,03C,05C)
- Intermittent operating equalizer/ampl. (06C)
- Broken cable/lack of power/faulty equalizer/amplifier (10C)

International Communication Circuits (London, SDAC)

The London CCT

Apart from minor irregularities, there was a reliable performance this period.

The SDAC Circuit

The performance of this circuit has been changing, and has been subject to tests quite frequently. These tests have been initiated by NCC (Network Control Center) but also by ITT. July was a quite good period with few irregularities. For August, however, the picture changed: 4, 5, 9, 10 and 20 August were affected by:

- Modem line test (NCC request)
- Loss of carrier
- Temporary line rerouting (NTA/Lillestrøm)
- Loss of carrier and frequently modem tests in different modes (NCC request)
- Modem check (4 hours), respectively.

The last month, September, has the following incidents:

1 September different line tests were requested by ITT after SDAC had claimed errors in data exchange with NORSAR. NTA and NDPC personnel were involved. According to indicators on the SDAC modem the line parameters were not outside specifications. 8 September the SDAC modem was put into "Audio

Bus Back" after NTA request, i.e., line loop in front of the modem at NDPC. 14 September message from NCC that line checks would be carried out in connection with introduction of a new "16 channel system", which, if successful, will improve the system's capability to handle more "packets" (messages).

O.A. Hansen  
J. Torstveit

TABLE II.3.1

Communications, degraded performance (>20)/outages (>200). Figures in per cent of total times. Month = 4 or 5 periods as indicated.

Sub-Array	July(5)		August(4)		September(5)	
	>20	>200	>20	>200	>20	>200
01A	0.4	0.6	0.4	0.1	0.2	0.2
01B	0.5	0.7	0.1	-	0.3	0.2
02B	0.3	0.6	0.1	-	0.4	0.3
03B	0.4	0.7	-	-	-	28.5
04B	0.3	0.7	0.1	0.2	0.6	0.2
05B	0.4	0.8	0.2	0.1	0.3	0.1
06B	18.4	3.3	0.4	0.3	0.4	1.3
07B	1.4	1.5	0.2	0.1	0.3	0.1
01C	8.3	57.9	0.2	0.1	0.2	0.3
02C	0.7	3.0	0.7	3.6	0.7	0.8
03C	0.3	0.7	0.2	0.3	1.0	8.3
04C	0.4	0.6	0.2	0.2	0.3	0.6
05C	0.5	0.5	4.2	2.8	0.4	1.6
06C	0.5	1.8	0.5	4.8	0.2	8.2
07C	-	0.2	-	-	-	-
08C	-	0.1	-	0.1	-	-
09C	1.0	1.7	0.2	0.3	0.4	0.2
10C	2.1	1.6	0.2	32.9	0.8	0.4
11C	11.1	1.9	7.5	0.2	15.6	0.1
12C	1.4	0.6	0.1	0.1	0.2	0.2
13C	1.1	0.2	0.1	0.1	0.2	0.2
14C	-	0.4	-	0.1	0.1	0.3
AVG.	3.2	3.6	0.7	2.1	1.0	2.4
Less	(01C)	1.0	(10C)	0.6	(03B)	1.1

II.4 ARPANET

There has been no change in the attachment configuration to, or use of, the NORSAR TIP since the last reporting period.

D. Rieber-Mohn

Category	Value	Value	Value	Value	Value
1.1	0.1	0.1	0.1	0.1	0.1
1.2	0.1	0.1	0.1	0.1	0.1
1.3	0.1	0.1	0.1	0.1	0.1
1.4	0.1	0.1	0.1	0.1	0.1
1.5	0.1	0.1	0.1	0.1	0.1
1.6	0.1	0.1	0.1	0.1	0.1
1.7	0.1	0.1	0.1	0.1	0.1
1.8	0.1	0.1	0.1	0.1	0.1
1.9	0.1	0.1	0.1	0.1	0.1
2.0	0.1	0.1	0.1	0.1	0.1
2.1	0.1	0.1	0.1	0.1	0.1
2.2	0.1	0.1	0.1	0.1	0.1
2.3	0.1	0.1	0.1	0.1	0.1
2.4	0.1	0.1	0.1	0.1	0.1
2.5	0.1	0.1	0.1	0.1	0.1
2.6	0.1	0.1	0.1	0.1	0.1
2.7	0.1	0.1	0.1	0.1	0.1
2.8	0.1	0.1	0.1	0.1	0.1
2.9	0.1	0.1	0.1	0.1	0.1
3.0	0.1	0.1	0.1	0.1	0.1
3.1	0.1	0.1	0.1	0.1	0.1
3.2	0.1	0.1	0.1	0.1	0.1
3.3	0.1	0.1	0.1	0.1	0.1
3.4	0.1	0.1	0.1	0.1	0.1
3.5	0.1	0.1	0.1	0.1	0.1
3.6	0.1	0.1	0.1	0.1	0.1
3.7	0.1	0.1	0.1	0.1	0.1
3.8	0.1	0.1	0.1	0.1	0.1
3.9	0.1	0.1	0.1	0.1	0.1
4.0	0.1	0.1	0.1	0.1	0.1
4.1	0.1	0.1	0.1	0.1	0.1
4.2	0.1	0.1	0.1	0.1	0.1
4.3	0.1	0.1	0.1	0.1	0.1
4.4	0.1	0.1	0.1	0.1	0.1
4.5	0.1	0.1	0.1	0.1	0.1
4.6	0.1	0.1	0.1	0.1	0.1
4.7	0.1	0.1	0.1	0.1	0.1
4.8	0.1	0.1	0.1	0.1	0.1
4.9	0.1	0.1	0.1	0.1	0.1
5.0	0.1	0.1	0.1	0.1	0.1
5.1	0.1	0.1	0.1	0.1	0.1
5.2	0.1	0.1	0.1	0.1	0.1
5.3	0.1	0.1	0.1	0.1	0.1
5.4	0.1	0.1	0.1	0.1	0.1
5.5	0.1	0.1	0.1	0.1	0.1
5.6	0.1	0.1	0.1	0.1	0.1
5.7	0.1	0.1	0.1	0.1	0.1
5.8	0.1	0.1	0.1	0.1	0.1
5.9	0.1	0.1	0.1	0.1	0.1
6.0	0.1	0.1	0.1	0.1	0.1
6.1	0.1	0.1	0.1	0.1	0.1
6.2	0.1	0.1	0.1	0.1	0.1
6.3	0.1	0.1	0.1	0.1	0.1
6.4	0.1	0.1	0.1	0.1	0.1
6.5	0.1	0.1	0.1	0.1	0.1
6.6	0.1	0.1	0.1	0.1	0.1
6.7	0.1	0.1	0.1	0.1	0.1
6.8	0.1	0.1	0.1	0.1	0.1
6.9	0.1	0.1	0.1	0.1	0.1
7.0	0.1	0.1	0.1	0.1	0.1
7.1	0.1	0.1	0.1	0.1	0.1
7.2	0.1	0.1	0.1	0.1	0.1
7.3	0.1	0.1	0.1	0.1	0.1
7.4	0.1	0.1	0.1	0.1	0.1
7.5	0.1	0.1	0.1	0.1	0.1
7.6	0.1	0.1	0.1	0.1	0.1
7.7	0.1	0.1	0.1	0.1	0.1
7.8	0.1	0.1	0.1	0.1	0.1
7.9	0.1	0.1	0.1	0.1	0.1
8.0	0.1	0.1	0.1	0.1	0.1
8.1	0.1	0.1	0.1	0.1	0.1
8.2	0.1	0.1	0.1	0.1	0.1
8.3	0.1	0.1	0.1	0.1	0.1
8.4	0.1	0.1	0.1	0.1	0.1
8.5	0.1	0.1	0.1	0.1	0.1
8.6	0.1	0.1	0.1	0.1	0.1
8.7	0.1	0.1	0.1	0.1	0.1
8.8	0.1	0.1	0.1	0.1	0.1
8.9	0.1	0.1	0.1	0.1	0.1
9.0	0.1	0.1	0.1	0.1	0.1
9.1	0.1	0.1	0.1	0.1	0.1
9.2	0.1	0.1	0.1	0.1	0.1
9.3	0.1	0.1	0.1	0.1	0.1
9.4	0.1	0.1	0.1	0.1	0.1
9.5	0.1	0.1	0.1	0.1	0.1
9.6	0.1	0.1	0.1	0.1	0.1
9.7	0.1	0.1	0.1	0.1	0.1
9.8	0.1	0.1	0.1	0.1	0.1
9.9	0.1	0.1	0.1	0.1	0.1
10.0	0.1	0.1	0.1	0.1	0.1

### III. ARRAY PERFORMANCE

Table III.1 shows some basic statistics for the EP operation during the present reporting period, in terms of analyst decisions for all the DP detections reported by EP. Table III.2 shows the number of reported events on a monthly basis, and in Fig. III.1 is shown the distribution on a daily basis. The numbers are quite normal, with an average of 20.7 events per day.

#### Complete Statistics 1971-76

The bulletin production under the full-sized NORSAR has now been discontinued, and it could therefore be interesting to look at the complete statistics up to 30 September 1976.

The EP processing statistics are given in Table III.3, where data are available from 1 July 1971. It is seen there that about 72 000 processings have been completed by EP, out of which 50%, or 36 000, have been accepted as true events. Note that the processing time was systematically decreased to a final value of about 15 minutes per event, with a corresponding decrease in the EP processing load on the B-computer. This increase in efficiency was the result of a systematic and concentrated effort on the part of the NTNF/NORSAR personnel in order to improve the processing packages and procedures originally developed and delivered by IBM/Federal Systems Division.

In Table III.4 we have given the number of reported events (teleseismic and core phases) for each year from 1 May 1971 to 30 September 1976. The reason why the total number (33809) is somewhat smaller than that given in Table III.3 for the number of accepted processings (35758) is that the latter sometimes includes several processed phases for the same event. It is seen that the overall average per day is 17.1, for the data after 1973 that number is 18.5.

H. Bungum

TABLE III.1

Analyst decisions for detections processed by EP during the time period July-Sept 1976

Analyst Classification	No. of Processings	Percentage
Accepted as events	2070	47.8
Rejected as being:		
- Poor SNR or noise	447	10.3
- Local events	713	16.5
- Double processings	559	12.9
- Communication errors	542	12.5
Sum Processed	4331	100.0

TABLE III.2

Number of teleseismic and core phase events reported during the time period July-Sept 1976

Month	Teleseismic	Core	Sum
July	557	122	679
Aug	623	135	758
Sept	366	102	468

TABLE III.3

Statistics of the total EP history from 1 July 1971 to 30 Sept 1976

Time Period	EP%	EP Hours	No. of Proc.	Time per Proc. (min)	No. of Acc. Proc.	Acceptance Percentage	Time per acc. event (min)
1971-2	37.9	1673	1706	58.8	971	56.9	103.4
1972-1	39.7	1736	4574	22.8	2913	63.7	35.8
-2	45.8	2023	8070	15.0	3729	46.2	32.6
1973-1	40.3	1749	7802	13.5	3899	50.0	26.9
-2	41.1	1815	8176	13.3	3478	42.5	31.3
1974-1	29.5	1283	7023	11.0	3298	47.0	23.3
-2	32.5	1434	7845	11.0	3798	48.4	22.7
1975-1	27.2	1175	7380	9.6	3929	53.2	17.9
-2	25.5	1128	6436	10.5	3214	49.9	21.1
1976-1	29.6	1292	8459	9.2	4459	52.7	17.4
-2	24.3	536	4331	7.4	2070	47.8	15.5
Sum		15844	71802		35758		
Daily Average	34.4	8.3	37.4	13.2	18.6		26.6

TABLE III.4

Number of events reported by NORSAR on a yearly basis, from 1 May 1971 to 30 Sept 1976

	Days	Teleseismic	Core Phase	Sum	Daily Average
1971	245	1674	568	2242	12.2
1972	366	5184	1009	6193	16.9
1973	365	5419	1169	6588	18.1
1974	365	4997	1337	6334	17.4
1975	365	5239	1265	6504	17.8
1976	274	4125	1823	5948	21.7
Sum	1980	26638	7171	33809	17.1

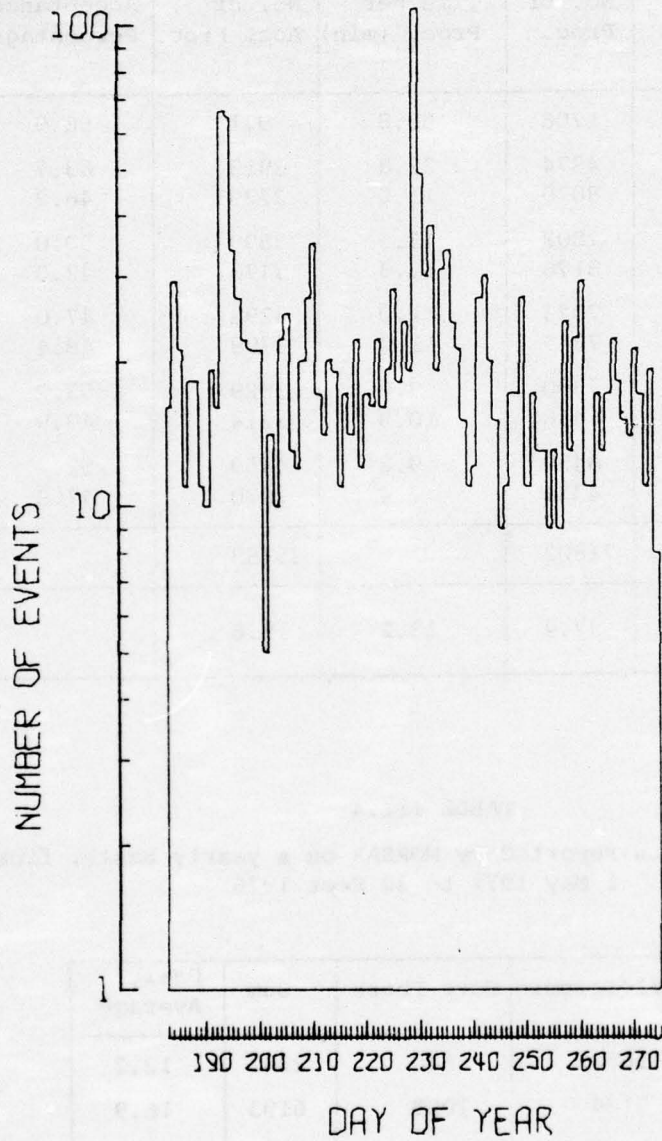


Fig. III.1 Number of events reported as a function of day of year, Jul-Sep 1976.

#### IV. IMPROVEMENTS AND MODIFICATIONS

##### IV.1 Detection Processor

Within this period, further modifications have been implemented in the Detection Processor system. These modifications fall into two categories:

- a. general error corrections and improvements,
- b. modifications to adapt the system to an environment with 7 subarrays only (versus 22 earlier).

Under a) the following changes were done to the system.

- The intra- and inter-task flow of ARPANET messages was considerably simplified. This was achieved by using one and the same queue block for a message for the duration of its flow through the system. In this way, the overhead of releasing and leasing queue blocks was reduced, and the algorithms became simpler.
- The handling of timed-out messages, waiting for acknowledgement (RFNM), was given to a separate subtask, which will be activated periodically, with intervals equal to the timeout period for messages sent out. Any stop in the flow of outgoing messages because of non-removal of timed-out messages should thus not occur.
- The problem of giving (internal) priorities to the various subtasks within the NCP task was finally solved, by adopting the principle of giving highest priority to subtasks with the lowest frequency of execution. In this way, high priority was given to the subtask handling timed-out messages (IMPTIM), the task-initialization-and-operator-message subtask (SNNCPR), and the Imp-to-Host command interpreter subtask (IMPHOS), while the subtasks handling the in- and outgoing ARPANET messages (IMPREAD, IMPIN, IMPOUT and IMPWRITE) got low priority. This setup seems to prevent any deadlock in the flow of ARPANET messages within the task.

- Numerous modifications have been made in other tasks, as queuing Incoherent Detections for ARPANET transmission, verification of tape start/stop times, removal of all code related to the EOC Beam Display (not used any more) and removal of all reference to the EOC debug tape.

Under b) the following changes and additions were made to the system.

- The PNRSPS processor, which reads the SPS block, was modified to read High Rate data from 14 subarrays only (this because 06C - the last subarray in the new configuration - is the 14th subarray in the old setup).
- The PNRNOR processor was modified to insert shortened 'manual' status fields from DP Global Common. Also, tests on instruments for DC offset, etc., will be performed on valid subarrays only.
- The PNRSAD processor, which sets up data messages for ARPANET transmission, was changed to extract status and data for the 7 valid subarrays only, for insertion into the transmission message block.
- The PNLRTP processor, which produces the Low Rate tape, was modified to call the subroutine LRXTRT, which extracts LP data from the High Rate block for the 7 valid subarrays, and builds a blocked Low Rate NR-record.
- The PNHRTTP processor, which produces the High Rate tape was modified to call the COMPRESS subroutine, which extracts SP data from the High Rate block for the 7 valid subarrays and builds a blocked High Rate 'NR'-record. This record will be written to tape when filled.
- A new subroutine LRXTRT (coded in PL360) was added to the tape task. This subroutine extracts LP status and data from integer second High Rate blocks, builds a Low Rate logical record, inserts this record into a physical record buffer and writes the buffer to tape when it is full and a write operation is possible.

- A new subroutine COMPRESS (coded in PL360) was added to the tape task. This subroutine extracts SP status and data from the current HR-block received from the Data Acquisition task, builds a compressed logical record and inserts this into the buffer for the High Rate 'NR' record.
- The PNRERR processor was modified to print the periodic Error Reports for valid subarrays only, and only if any of the error counts for the passed interval were non-zero.
- The size of the largest queue block, defined in RMONCOMS, was reduced from 1250 to 775 FWs. This could be done because the latter size was adequate for the transportation of HR-data from 14 SAs through the system (instead of 22).
- A separate, fixed buffer capable of storing up to 4 compressed logical HR records before the write operation, was added to the system (HRBUFFS).

D. Rieber-Mohn

#### IV.2 Event Processor

No modifications were done to the EP system during this period.

D. Rieber-Mohn

### IV.3 Array Instrumentation

The project described in the last semiannual report (1 January-30 June 1976) of running a three-axis SP seismometer at subarray 14C has continued with good results, except for noise on the Z-component data, LF oscillations in the period 24 July to 5 August due to water in the seismometer plug and superimposed 50 Hz noise, corrected 24 August. As previously, channel 03 and the LP channels at 14C have been attenuated 30 dB, and channel 14C05 has been used for phase shift reference (Section VII.1, this report). The lowpass active filter at the LTAs were bypassed on the channels 14C01, 02, 04 and 06 in this period.

The array reduction program started in September with cutting and plugging of the CTV air pipes on five sites.

In the new array configuration attenuated LP channels are planned. If a sampling rate of every two seconds are sufficient, it is possible to sample the output from the three LP seismometers at a site in parallel, by feeding the (attenuated) signal to random data addresses (RDA) 13, 14 and 15 for vertical, NS and EW respectively. It was technically checked out at 01B from 15 September, by feeding NS seismometer data output to RDA13.

Alf Kr. Nilsen

V. MAINTENANCE ACTIVITY

This section includes a review of the maintenance accomplished at the subarrays by the field technicians as a result of the remote array monitoring and visual inspections. There are no changes in the monitoring schedule this period, but due to frequent EOC and DP faults the schedule has been only loosely followed.

Maintenance Visits

Fig. V.1 shows the number of visits to the subarrays in the period. Excluding visits caused by troubles in the communication system, the subarrays have on the average been visited 2.8 times (excluding 01A and 06C: 2.1 times). The large number of visits to 01A are due to painting of the LPV and cable breakages, at 06C due to troubles with the SLEM and cable breakage.

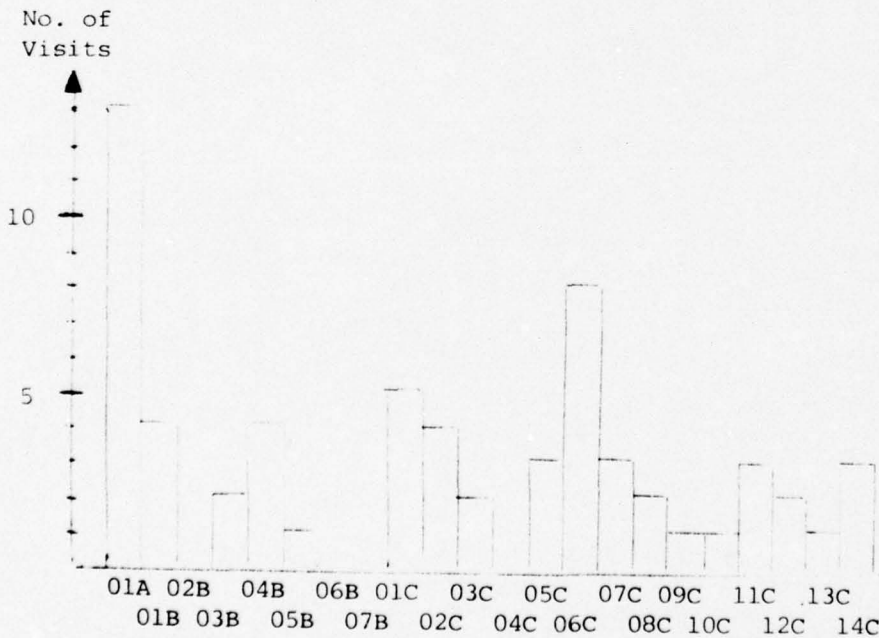


Fig. V.1 Number of maintenance visits to the NORSTAR subarrays  
1 July - 30 September 1976.

Preventive Maintenance Projects

The preventive maintenance work in the array is described in Table V.1.

TABLE V.1

Unit	Action	No. of Actions		Comments
		Accomp.	Remaining	
LTA	Adjustment of SP DC offset	11		
	Adjustment of channel gain SP	7		
	Adjustment of channel gain LP	1		
Power	Battery Maintenance	3		
LPV	Painting of LPV*	2	0	01A, 02C

\* Reported as corrective maintenance in the montly reports due to the great need for this work, but have preventive effects as well.

Disclosed Malfunctions on Instrumentation and Electronics

Table V.2 gives the number of accomplished adjustments and replacements of field equipment in the total array with the exception of those mentioned in Table V.1.

TABLE V.2

Total number of required adjustments and replacements in the NORSAR data channels and SLEM electronics

Unit	Characteristic	SP		LP	
		Repl.	Adj.	Repl.	Adj.
Seis- mometer	Sensitivity				2
	RCD			3	13
Seis- mometer Ampli- fier (RA-5)	Taper pin block	1			
	Protection card	2			
LTA	Ch gain		12		5
BE Card		1			
SLEM					
BB gen.			2		
RSA/ ADC			1		
EPU		1	1		
DU		1			

Malfunction of Rectifiers, Power Loss, Cable Breakages

Malfunction of the rectifiers and power loss requiring action of the field technicians or local power company are reported in Table V.3.

TABLE V.3

Faults disclosed in subarray rectifiers and power loss

Sub-Array	Fault	Period of Inoperation	Comments
01C	No power at site --	8-9 July 12-12 July 15-31 July	Rectifier did not re-start after AC power break. EPU converter card faulty.
06C	Noise on data	10-22 Sept.	EPU and DU replaced
10C	No power at site	12-13 Aug	Blown main fuses and one fuse in battery charger
12C	No power to MP lamps		4v Oltronic power supply replaced.

Nine cable breakages have been repaired, or attempts to repair have been made, requiring 17 days' work of the field technicians. Due to the short time left before reduction of the array, the repairs were not completed at 04B02 and 07C03. At 01A04 the cable repair was dropped, as we intend to use this channel for attenuated SP data.

Conclusion

The performance of the array instrumentation has been satisfactory in the period and compared with previous periods no anomalies in the operation were observed.

Two power supplies of NORSAR analog SP station (NMC/04B05) were damaged by lightning 10 July. Difficulties in acquiring spare parts have caused inoperation from that date and out the period.

A. Kr. Nilsen

ABBREVIATIONS

AC	-	Alternate current
ADC	-	Analog-to-Digital Converter
BB	-	Broad band
BE card	-	Lightning protection card
CMR	-	Common mode rejection
CTV	-	Central Terminal Vault
DC	-	Direct current
DP	-	Detection processor
DCO	-	DC offset
DU	-	Digital unit
EOC	-	Experimental Operations Console
EPU	-	External power unit
LF	-	Low frequency
LP	-	Long period
LPV	-	Long period vault
MP	-	Mass position
NMC	-	NORSAR Maintenance Center
RA-5	-	SP seismometer amplifier
RCD	-	Remote centering device
RSA	-	Range switching amplifier
SLEM	-	Seismic short and long period electronics module
SP	-	Short period
WHV	-	Well head vault

VI. DOCUMENTATION DEVELOPED

VI.1 Reports, Papers

Berteussen, K.-A. (1976): Semiannual Technical Summary, Sci. Rep. No. 4-75/76, NTN/NORSAR, Kjeller, Norway.

Berteussen, K.-A. (1976): Direct measurement of crustal P-velocities in the NORSAR area, submitted for publication.

Bungum, H., and E.S. Husebye (1976): Seismicity of the Norwegian Sea: Jan Mayen Fracture Zone, Tectonophysics (in press).

Husebye, E.S., H. Bungum, J. Fyen and H. GjØystdal (1977): Earthquake activity in Fennoscandia between 1497 and 1975 and intraplate tectonics, Norske Geologiske Tidsskrift, (in press).

Ringdal, F., and H. Bungum (1976): Noise level variation at NORSAR and its effect on detectability, submitted for publication.

L.B. Tronrud

VI.2 Program Documentation

No program documentation has been written during this period.

D. Rieber-Mohn

VII. SUMMARY OF SPECIAL TECHNICAL REPORTS/PAPERS PREPARED

VII.1 Seismic Velocity Variations and Solid Earth Tides

We have previously (Final Technical Report, 1 July 1974-30 June 1975; Semiannual Technical Report 1 July - 31 December 1975) reported on this project, in which 2.778 Hz monochromatic waves from a hydroelectric power plant have been used for precise monitoring of seismic velocities. It has been found that precisions of the order of  $10^{-3}$  are obtained when 2 hours of data are stacked, and  $10^{-4}$  with 7 days of data. The average group velocity is around 3.5 km/s.

In order to determine the wave type that we are observing, a three-component set of short period seismometers was installed in site 14C02, 4.7 km away from the source. The particle motion was then derived by application of Fourier analysis and stacking, where relative amplitudes and phase delays were used in the actual constructions of the plot, as shown in Fig. VII.1.1. It is seen there that the radial to transverse amplitude ratio is so small that only S-waves can satisfactorily explain the observations. This solution is also consistent with the velocity observations around 3.5 km/s.

A systematic search for periodicities in the data has revealed the presence of velocity variations with a cycle time of 12 hours. This is shown in Fig. VII.1.2, where the two full cycles in the 24 hours plot demonstrate that we are not observing a hidden diurnal component (such as a non-symmetric temperature effect). We have searched the data for a number of other periods too, and find a response for periods in the range of 11-13 hours. This of course should be expected when only 7 days of data have been analyzed, but it is noteworthy here that the measured phase delays for the different periods in the 11-13 hours range are found from simulation analysis not to be consistent with leakage from a single spectral component.

The closest place to look for a source of these velocity variations is in the earth tidal field, which has been calculated theoretically through the harmonic expansion of the tide-generating potential of second order. In this way, the horizontal components of the strain tensor have been calculated for the time periods in question, but no correlation has been found with the observed velocity variations, with the important exception that the periods coincide. This lack of correlation so far as initial phase is concerned does not, however, exclude the possibility of a tidal source. This is because there are factors such as ocean loading and atmospheric pressure variations which have not been taken into consideration in the theoretical calculations. More important, however is the doubt that we have as to the assumption of a direct relationship between velocity and strain, this is partly because the (unknown) distribution in direction and size of the cracks in the material also enters this relationship.

The velocity variations displayed in Fig. VII.1.2 are of the order of  $10^{-3}$ . The predictions here, based on extrapolation of laboratory values, give values of the order of  $10^{-5}$ . If the velocity variations that we observe are actually caused by earth tides, this therefore means that there is a very high velocity sensitivity to stress variations in the uppermost layer of the earth.

H. Bungum  
T. Risbo  
E. Hjortenbergt

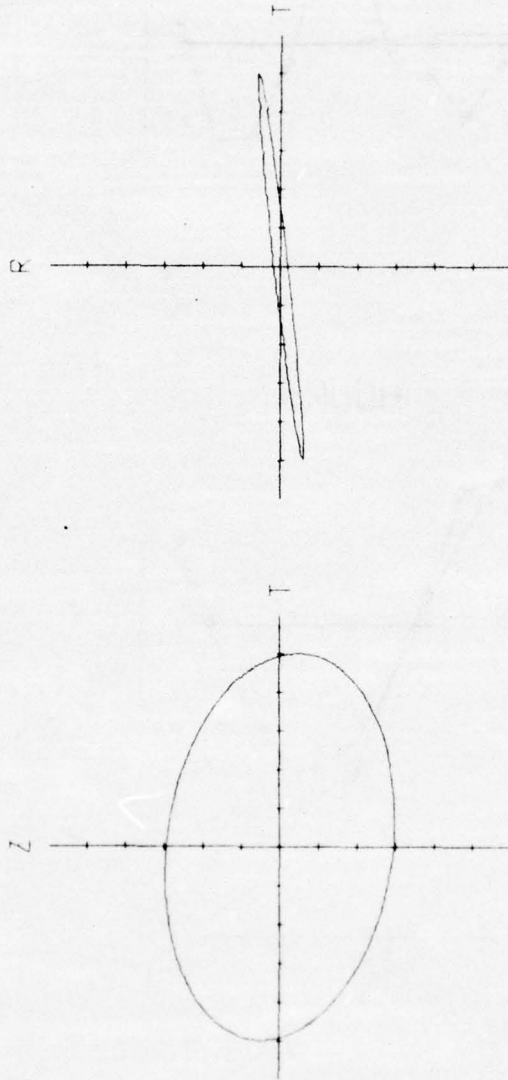


Fig. VII.1.1.1 Particle motion plot of the 2.778 Hz monochromatic waves as recorded 4.7 km away from the source. The solution is based on about 10 hours of data.

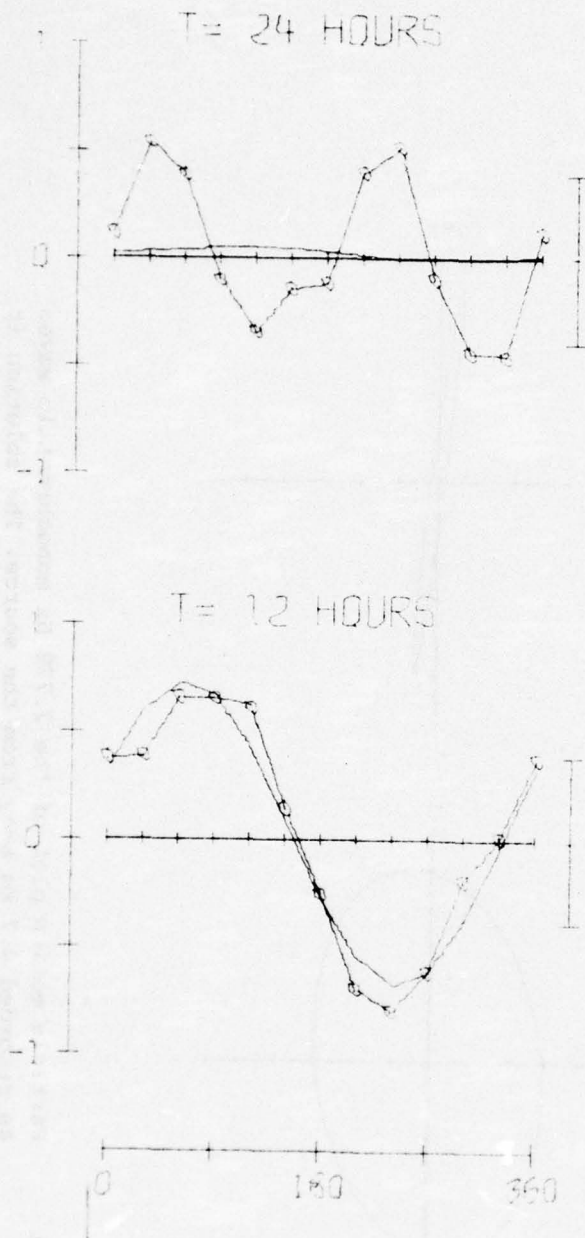


Fig. VII.1.2 Propagational phase angle differences when measured with a sliding window procedure in such a way that the presence of the searched-for periodicity should show up in the form of a one cycle sine wave. This is the case for  $T=12$  hours, while it is the 12 hours periodicity which shows up as two cycles on the plot for  $T=24$  hours.

## VII.2 Weighted Beamforming using Non-negative Weights

Considerable attention has been given to the weighted beamforming process of Christoffersson and Husebye (1974), where negative weights were allowed. Fyen et al (1975) showed that the presence of negative weights permitted additional statistical tests for use by the analyst in the signal-noise classification. The weights used in this beamforming process arose from the model

$$y_j = \gamma_j S + n_j \quad j = 1, \dots, M \quad (1)$$

where  $y_j$  is the recorded data at sensor  $j$ ,  $S$  is the unknown signal and  $\gamma_j$  an unknown scaling factor which accounts for the observed amplitude variation at NORSAR.  $n_j$  is the residual noise of the model. The least squares estimators of this model are

$$\hat{S} = \sum \hat{\gamma}_j y_j \quad (2)$$

where  $\hat{\gamma}_j$  are the elements of the eigenvector corresponding to the largest eigenvalue of the matrix  $y'y$ , i.e., the variance-covariance matrix of the recordings (first principal component).

When  $\hat{\gamma}_j$  takes negative values, it means physically that the sensor output has a phase shift of  $\pi$  relative to the beam. This in turn could occasionally lead to undesirable side effects as the phase shift option may result in projection of pure noise wavelets into the signal space. A project was therefore carried out where the estimated weights were permitted to take non-negative values only. The method of least squares leads to minimizing

$$F = \sum_{j=1}^M (y_j - \gamma_j S)' (y_j - \gamma_j S) - \lambda \left( \sum_{j=1}^M \gamma_j^2 - 1 \right) \quad (3)$$

where  $\lambda$  is the Lagrangian multiplier reflecting the restriction  $\sum_{j=1}^M \gamma_j^2 = 1$ . The minimum of  $F$  is found by an iteration procedure where only  $\gamma \geq 0$  is permitted. This gives the same solution as the principal component method when all  $\gamma_j > 0$  are positive. However, when some of the  $\gamma_j$  took negative values, the iteration procedure will give a solution which gives zero weights to sensors out of phase and slightly different values for others.

The procedure was applied to a set of mostly weak earthquakes with varying signal-to-noise ratios and extreme noise cases which trigger the on-line detector (false alarms). The results showed that non-negative weights do not give an opportunity to create additional statistical tests for signal-noise classification. However, when calculating signal-to-noise (SNR) ratios, the analysis showed that non-negative weights preserve the same SNR as the principal component procedure, and for extreme noise cases the SNR is reduced by at least 0.15 units on an average. In this region of SNR we know that the number of detections increases exponentially with decreasing SNR, so a reduction of SNR for extreme noise of 0.15 units is considered as a significant improvement relative to principal component beams, in terms of an SNR detector.

J. Fyen

A. Christoffersson, Uppsala

#### References

- Christoffersson, A., and E.S. Husebye (1974): Least squares estimation techniques in analysis of seismic array recorded P-waves, *Geophys. J.R. Astr. Soc.*, 38, 525-552.
- Fyen, J., E.S. Husebye and A. Christoffersson (1975): Statistical classification of weak seismic signals and noise at the NORSAR array, *Geophys. J.R. Astr. Soc.*, 42, 529-546.

### VII.3 Long Period P-Wave Spectra as a Tool for Studies of Local Structure

The vertical (Z) and horizontal-radial (R) signal spectra for a body wave may be written

$$Z = S \cdot H_Z \cdot I + N_Z \quad (1)$$

$$R = S \cdot H_R \cdot I + N_R \quad (2)$$

where S is the source and the source-side effects,  $H_Z$  ( $H_R$ ) is vertical (horizontal) transfer function of the crust and upper mantle on the receiver side, I is instrument response and  $N_Z$  ( $N_R$ ) is noise on the vertical (horizontal) component. All the above parameters are a function of the angular frequency. Assuming  $N_Z = N_R = 0$  one may form the ratio

$$G = Z/R = H_Z/H_R \quad (3)$$

Phinney (1964) originally proposed the idea of dividing the spectra of the vertical component of a recorded P-wave with that of the horizontal radial component in this way, thereby obtaining a ratio which does not depend on the spectrum of the original incident pulse. These ratios are then compared with theoretical layered models using the Haskell (1953)-Thomson (1950) matrix theory. This 'spectral ratio' method has since been used by a large number of authors.

The aim of this work (Berteussen, 1976a) has been to find out what type of information one may expect to get about the structure under a station (having a three-component long period instrument set) by applying this spectral ratio method. To do this we have used only simulated data, while we in a later work (Berteussen, 1976b) also will try real data from the three-component long period instruments at the Norwegian Seismic Array (NORSAR).

Simulating a number of different models, we have found that by far the most pronounced effect on the spectral ratio is caused by the Moho boundary. For this boundary the effect of, for example, changing the depth is very obvious and can easily be seen on the simulated ratios. Other interfaces may complicate the picture, like for example enlarging one of the peaks caused by the Moho boundary, but it is extremely difficult without other evidence to assign these additional effects to a particular model (Fig. VII.3.1 and VII.3.2). For example, interfaces at 10 km depth and 30 km depth can give rise to almost the same set of peaks. Compare trace 4 from top on Fig. VII.3.1) with traces 4 and 6 on Fig. VII.3.2. Structures below Moho may give a large number of additional smaller peaks (top traces Fig. VII.3.4), but neither of these structures seem able to change drastically the spectral ratio generated by the Moho boundary. Also it may be difficult even for a one-layer case to discriminate between a deep crust with high velocity and a shallow one with lower velocity (Fig. VII.3.3). By taking into account also the size of the spectral peaks, this should, however, be possible although the peak sizes are easily affected by noise.

When using Fourier theory to estimate the vertical and horizontal spectra, we will have to use a time window of a certain length. The estimated ratio is then (a star means convolution)

$$\hat{G} = \frac{Z * W}{R * W} = \frac{(S \cdot H_Z \cdot I + N_Z) * W}{(S \cdot H_R \cdot I + N_R) * W} \quad (4)$$

Since convolution is an integral operation, we can in general not cancel the common terms in the numerator and denominator in Eq. (4), even if we assume  $N_Z = N_R = 0$ . In the practical estimation of the spectral ratios, one has to ensure that a long enough window is used in the calculation of the spectra (see Fig. VII.3.4). For the type of instruments used at NORSAR this means 50 seconds or longer, but with other instruments with a

flatter response curve a somewhat shorter window may be used, although as demonstrated a 20 second window is surely too short. If one would like to see the full effect of the upper mantle on these ratios, a window of up to 180 sec is needed. There are several other factors to be aware of. One needs signals with very good signal-to-noise ratio, and the signal should be as pulse-like as possible. A very deep source is to be preferred (one thereby may avoid any source-side depth phases), but is not a completely necessary requirement. It is found that depth phases are only a problem when they are so strong and arriving so late that they may be seen on the record. By selecting only simple pulse-like signals one therefore can avoid this problem.

In short, from the simulations performed we conclude that one can use the spectral ratio method to find the depth to Moho if proper care is taken in the data processing. We do not believe that it is possible to find a more detailed model, at least not without any other evidence.

K.-A. Berteussen

References

- Berteussen, K.-A. (1976): Long period P-wave spectra as a tool for studies of local structure, manuscript in preparation.
- Berteussen, K.-A. (1976b): Moho depth determination based on spectral ratio analysis of NORSAR long period P-waves, manuscript in preparation.
- Haskell, N.A. (1953): The dispersion of surface waves on multilayered media, Bull. Seism. Soc. Am., 43, 17-34.
- King, D.W., and G. Calcagnile (1976): P-wave velocities in the upper mantle beneath Fennoscandia and Western Russia, Geophys. J.R. Astr. Soc., 46, 407-432.
- Phinney, R.A. (1964): Structure of the earth's crust from spectral behavior of long period body waves, J. Geophys. Res., 69, 2997-3017.
- Thomson, W. (1950): Transmission of elastic waves through a stratified medium, J. Appl. Phys., 21, 89-93.

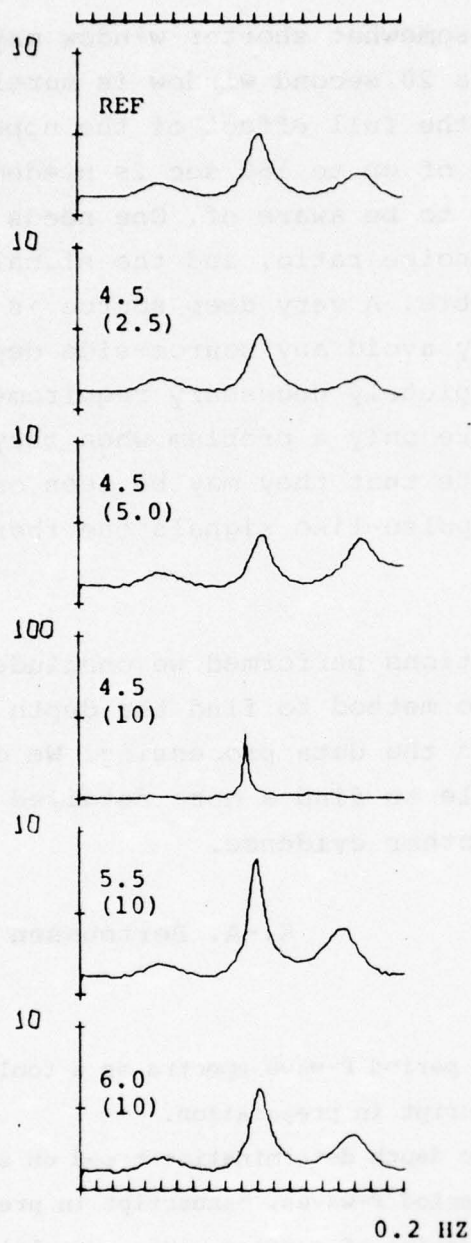


Fig. VII.3.1 Illustration of the effect on the theoretical spectral ratio of low velocity surface layers. In the first trace is plotted the ratio for a one-layered reference model with crustal P-velocity equal to 6.6 km/sec and Moho depth 35 km. In the following cases are then plotted the ratios for different cases of surface layers. The thickness of the layer and its P-velocity (in brackets) is written on the figures.

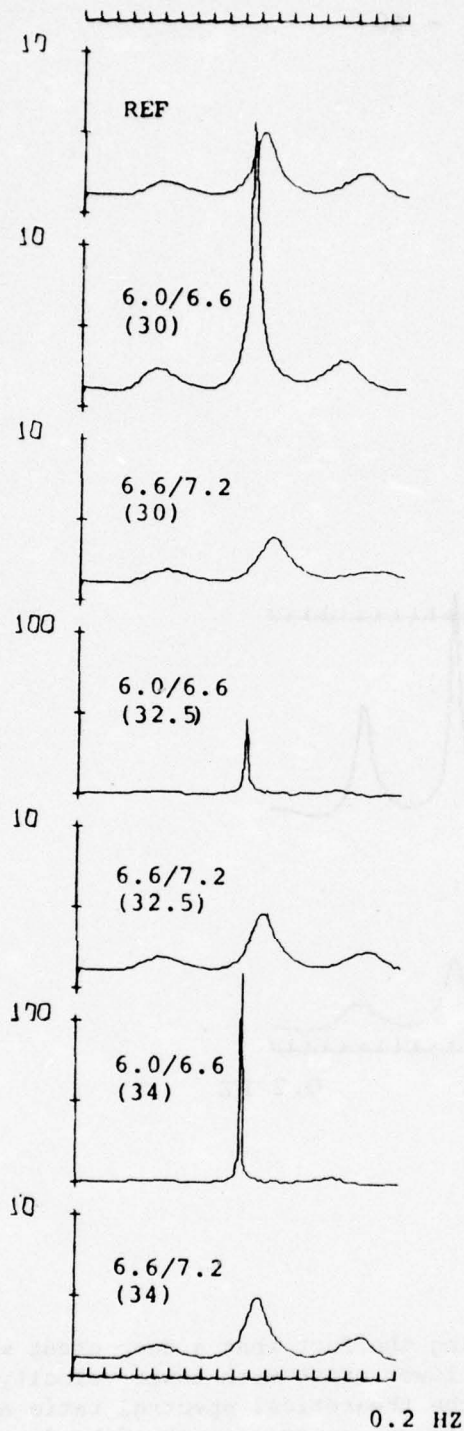


Fig. VII.3.2 Illustration of the effect on interfaces in the deeper part of the crust. As before the upper trace is the spectral ratio for a one-layered 35 km thick reference model, while the other traces are for different types of two-layered models. The depth (in brackets) of the intermediate interface and the P-velocity above and below it are given on the figure.

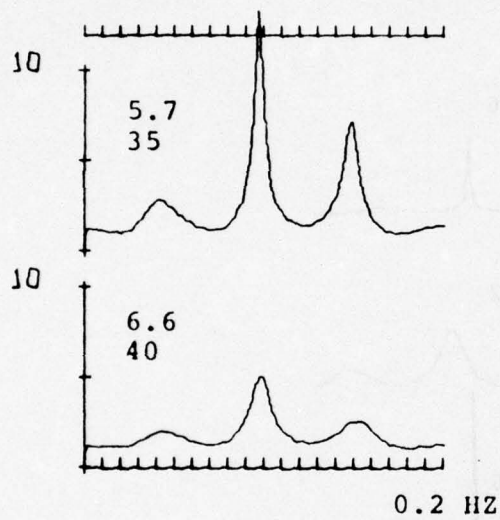


Fig. VII.3.3 Illustrating the fact that a deep crust with high velocity and a shallower crust with lower velocity will have the peaks in the theoretical spectral ratio at the same frequencies. In the upper case the Moho depth is 35 km and the crustal P-velocity is 5.7 km/sec, while in the lower case the corresponding numbers are 40 km and 6.6 km/sec.

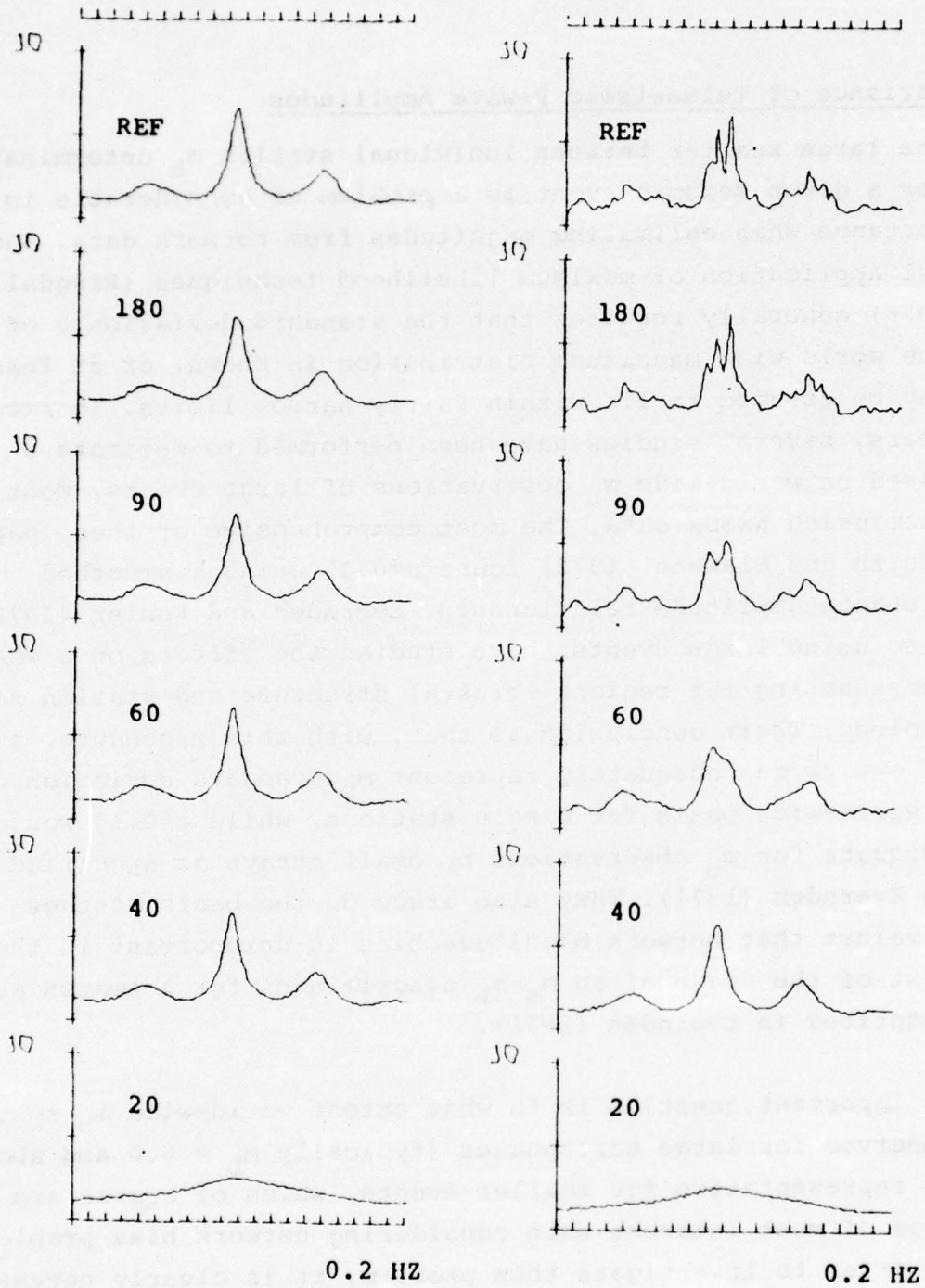


Fig. VII.3.4 Illustration of the effect of different window length in the calculation of the spectral ratio. The model used is the crustal model (left panel) and the whole crust and upper mantle model of King and Calcagnile (1976). The top trace in both cases is the theoretical ratio, while the other traces give the ratio that will be observed for different lengths of the Fourier window. Window length in seconds is given on the figure. The source function, the source-side crust response the effect of the mantle as well as the effect of the instrument response have been ignored in the calculations.

#### VII.4 Variance of Teleseismic P-wave Amplitudes

The large scatter between individual station  $m_b$  determinations for a given seismic event is a problem of considerable importance when estimating magnitudes from network data. Successful application of maximum likelihood techniques (Ringdal, 1976) generally requires that the standard deviation  $\sigma$  of the world-wide magnitude distribution is known, or at least may be assumed to lie within fairly narrow limits. In recent years, several studies have been performed to estimate  $\sigma$  based on world-wide  $m_b$  observations of large events, most of them using WWSSN data. The most comprehensive of these papers (Veith and Clawson, 1972) found  $\sigma=0.35$  using a smoothed distance-amplitude relationship. Evernden and Kohler (1976), also using large events, have studied the effects on  $\sigma$  when compensating for regional crustal structure and station site geology. Their conclusion is that, with this procedure, a value of  $\sigma=0.21$  can adequately represent  $m_b$  standard deviation on a world-wide basis for single stations, while  $\sigma=0.15$  would be adequate for  $m_b$  observations by small arrays as specified in Evernden (1971). They also argue on the basis of these low  $\sigma$  values that network magnitude bias is unimportant in the context of the usage of an  $M_s-m_b$  discriminant for networks as described in Evernden (1971).

An important question is to what extent world-wide  $m_b$  scattering observed for large earthquakes (typically  $m_b = 6.0$  and above) is representative for smaller events, which of course are the ones of most interest when considering network bias problems. In order to investigate this problem, it is clearly necessary to employ another procedure than looking at world-wide magnitudes of a given event. This is because the problem of non-detections at individual stations becomes quite severe with existing earthquake catalogues for low-magnitude events. Instead, we choose in this paper the indirect approach of comparing  $m_b$  values of the large arrays LASA and NORSAR for events from selected regions, assuming independence of their respective  $m_b$  estimates.

The results of this analysis are presented in Table VII.4.1, and show that the scatter is significant and appears to be quite region-dependent. For the six geographic regions analyzed, we have estimated an average  $\sigma=0.30 m_b$  units for the standard deviation around the 'true' magnitude of each array  $m_b$ . At individual regions,  $\sigma$  ranges from 0.21 (Central America) to 0.40 (Kurile Islands) - see also Fig. VII.4.1. It should be noted here that any systematic regional station bias, including average signal attenuation effects due to local site geology, have been eliminated prior to computing the variances. It appears that the scatter could be reduced if smaller regions are considered; however, it might be noted that Ringdal (1974) found a value of  $\sigma$  as high as 0.28 for an aftershock sequence from the Kurile Islands 17-30 June 1973, comparing NORSAR and LASA reported  $m_b$  values. Hence, a significant residual scatter remains, even when very small source areas are considered.

Our  $\sigma$  estimates are significantly higher than those of Evernden and Kohler (1976). This may reasonably be attributed to the difference in spectral characteristics of large and small earthquakes, i.e., smaller earthquakes tend to have a relatively higher corner frequency (Aki, 1967). In fact, Fig. VII.4.2 shows the standard deviation of log amplitudes across the NORSAR array in five frequency bands (each of bandwidth 0.4 Hz). The data represent average values of 10 events, listed in Table VII.4.2. A clear increase in amplitude scattering is observed with increasing frequency, with a standard deviation at 2 Hz almost double that at 0.6 Hz.

Hence, these results indicate that world-wide  $m_b$  scatter increases with decreasing magnitudes, and thus that magnitude bias studies based on large events will not necessarily be adequate at low magnitudes.

F. Ringdal

References

- Aki, K. (1967): Scaling law of seismic spectrum, J. Geophys. Res., 72, 1217-1231.
- Evernden, J.F. (1971): Location capabilities of various networks, Bull. Seism. Soc. Am., 61, 241-273.
- Evernden, J.F., and W.M. Kohler (1976): Bias in estimates of  $m_b$  at small magnitudes, to be published.
- Flinn, E.A., E.R. Engdahl and A.R. Hill (1974): Seismic and geographical regionalization, Bull. Seism. Soc. Am., 64, 771-993.
- Ringdal, F. (1974): Estimation of seismic detection thresholds, Report No. Alex(01)-TR-74-02, Texas Instruments Inc., Dallas, Texas.
- Ringdal, F. (1976): Maximum-likelihood estimation of seismic magnitude, Bull. Seism. Soc. Am., 66, 789-802.
- Veith, K.F., and G.E. Clawson (1972): Magnitude from short-period P-wave data, Bull. Seism. Soc. Am., 62, 435-452.

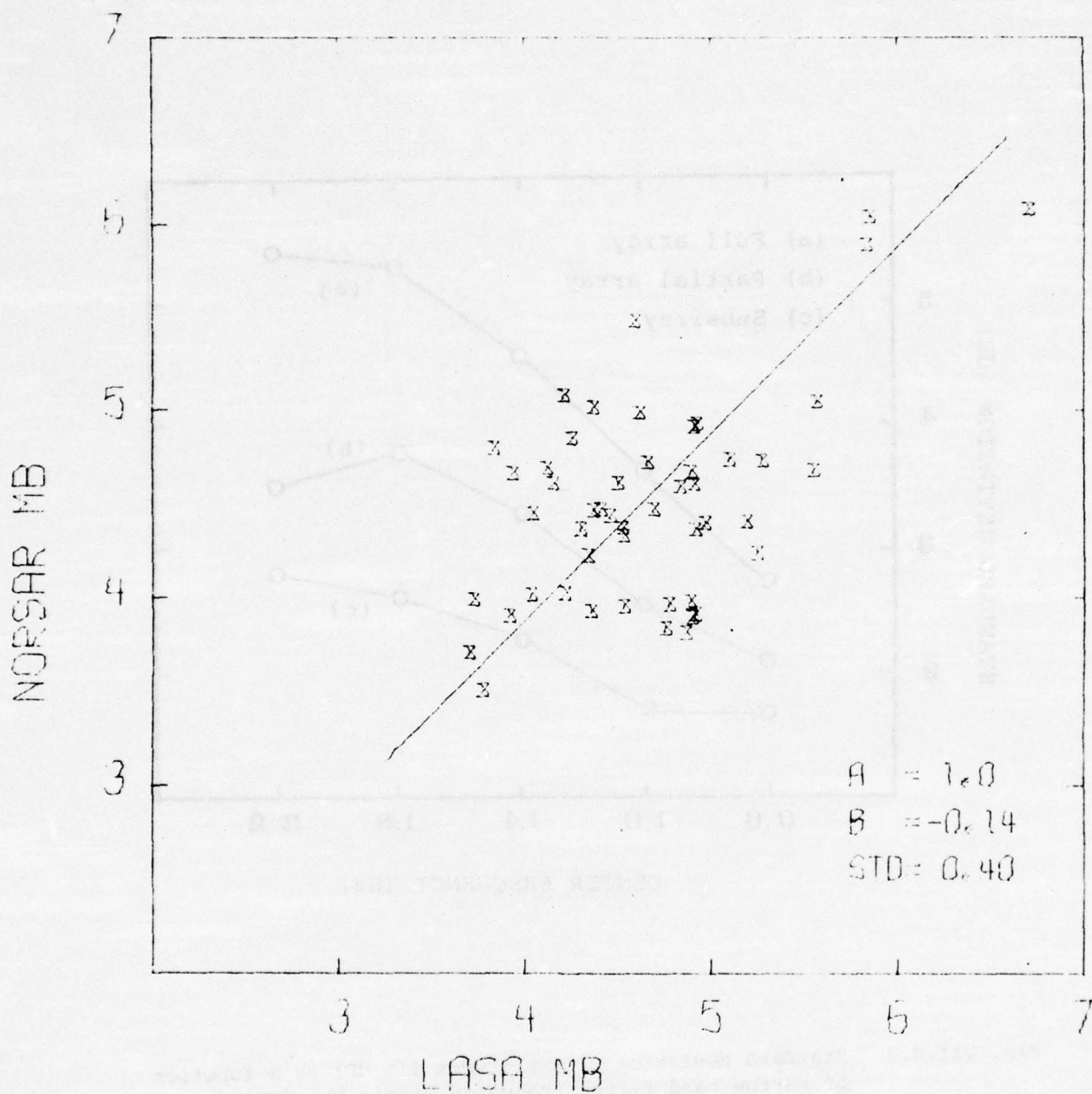


Fig. VII.4.1 Comparison of NOR SAR and LASA reported  $m_b$  for 50 events randomly selected from the Kurile Islands area (Flinn-Engdahl regions 220-222). The straight line has a slope of  $A=1.0$ , and its intercept  $B$  (denoting the average difference  $m_b(\text{NOR SAR}) - m_b(\text{LASA})$ ) and the orthogonal standard deviation relative to this line are also specified.

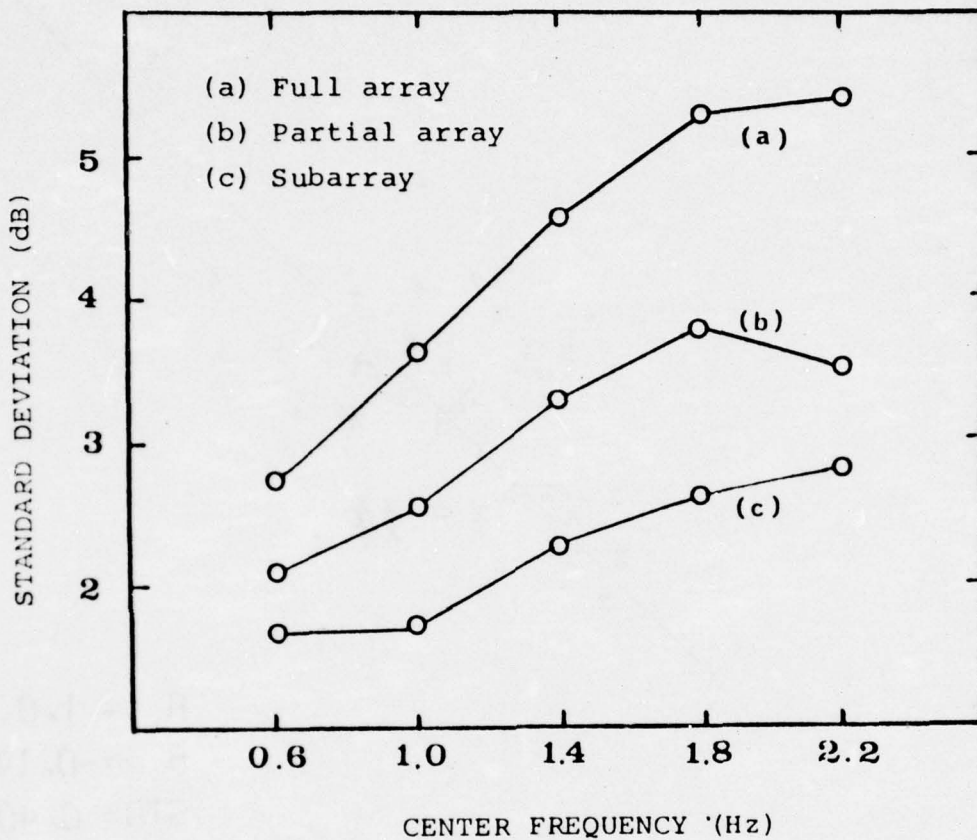


Fig. VII.4.2 Standard deviation of amplitudes (in dB) as a function of narrow-band filter frequency within the NORSAR array (a), within a partial array consisting of three neighboring subarrays (b) and within a subarray (c). The numbers represent average values over a set of 10 events.

TABLE VII.4.2  
Events used for studying NORSAR amplitude variations.

Event No.	Region	Reported by PDE				Reported by NORSAR					
		Date	Origin Time GMT	Latitude	Longitude	Depth	$m_b$	T (S)	Dist (deg)	Azi (deg)	
1	Afghanistan-USSR Border	06/26/71	22.23.29	36.3N	71.4E	127	5.0	5.3	0.5	45	95
2	Eastern Kazakh SSR*	06/30/71	03.56.57	50.0N	79.1E	0	5.4	5.2	1.0	40	77
3	Szechwan Province, China	08/16/71	04.58.00	28.9N	103.7E	N	5.5	5.6	1.0	64	75
4	Honshu, Japan	04/26/75	03.14.37	39.6N	141.1E	100	5.3	5.3	0.3	72	45
5	South of Honshu, Japan	05/06/75	10.18.20	31.0N	141.7E	N	5.7	5.6	0.7	81	49
6	Southern Nevada*	06/03/75	14.40.00	37.3N	116.5W	0	5.7	5.6	1.2	72	323
7x	Kirgiz-Sinkiang Border	03/16/76	06.19.09	41.0N	77.0E	N	-	5.2	0.7	44	88
8x	Kurile Islands	04/03/76	19.14.17	45.0N	149.0E	N	-	4.9	0.8	69	35
9x	Uzbek, SSR	04/08/76	12.03.59	42.0N	62.0E	N	-	5.2	0.9	36	98
10x	Off Coast Hokkaido, Japan	04, 11/76	02.52.50	43.0N	147.0E	N	-	5.4	0.7	71	38

\* Presumed explosion

x All parameters reported by NORSAR

TABLE VII.4.1  
Regional statistics of LASA-NORSAR magnitude differences.

General Region	Corresponding Flinn-Engdahl Regions	Number of Events	Average $m_b(\text{LASA}) - m_b(\text{NORSAR})$	St. dev. of $m_b(\text{LASA}) - m_b(\text{NORSAR})$	St. dev. of each array $m_b$
S. Honshu	226-233	50	0.03±0.04	0.31±0.03	0.22±0.02
Kurile Islands	220-222	50	0.14±0.08	0.56±0.06	0.40±0.04
Kamchatka	217-219	50	-0.04±0.06	0.39±0.04	0.27±0.03
Aleutian Islands	4-10	50	0.05±0.07	0.46±0.05	0.33±0.03
North Atlantic Ridge	402,403,406	50	-0.08±0.07	0.46±0.05	0.32±0.03
Central America	54-82	50	-0.09±0.04	0.30±0.03	0.21±0.02
All above regions combined		300	0.00±0.03	0.42±0.02	0.30±0.01

APPENDIX A

FORMAT OF THE NORSAR HIGH RATE DATA TAPE EFFECTIVE 1 OCTOBER 1976

1. INTRODUCTION

This note describes a new format for the NORSAR High Rate (HR) tape, capable of accepting data from maximum 7 subarrays. This format is valid from 1 October 1976.

2. THE NEW 'HR' RECORD FORMAT

Each physical record on the HR-tape will consist of 4 HR-blocks, the first one having an integer second time. Each block will have the following format (see Figure 1).

- A set of control fields constituting 62 bytes
- 5 logical records, each of 262 bytes.

This will give a block size of 1372 bytes and a physical record length of 5488 bytes. Details of the component fields follows below:

		<u>Field</u>
<u>Bytes 0-1</u>	Record Id "NR"	0
<u>Bytes 2-5</u>	Binary ISRSPS time	1
<u>Bytes 6-7</u>	General Indicators	2
Bits 0-2	spare	
"	3 TOD failure, interpolated time supplied	
"	4 change in Field 3 status	
"	5 " " " 4 "	
"	6 " " " 5 "	
"	7 " " " 6 "	
"	8-15 spare	

PRECEDING PAGE BLANK-NOT FILMED

		<u>Field</u>
<u>Bytes 8-9</u>	Automatic Subarray Status	3
	2 bits per subarray, according to the following code:	
	01: all sequential channels invalid	
	10: all submultiplex channels invalid	
	11: all channels invalid or subarray not defined	
	00: non of the above (i.e., OK).	
	2 bits per subarray gives 14 bits for 7 subarrays, bits 14-15 will be set to 11.	
<u>Bytes 10-30</u>	Automatic Seismometer Status	4
	24 bits per subarray, according to the following code:	
	Bit 0-5: 1 bit for each <u>sequential</u> channel. Bit set denotes invalid channel	
	8-23: 1 bit for each <u>submultiplex</u> channel. Bit set denotes invalid channel.	
	7 subarrays occupy 21 bytes.	
<u>Bytes 31-32</u>	Manual (on-line) Subarray Status	5
	2 bits per subarray, as for Field 3 (2 unused bits, set to 11)	
<u>Bytes 33-53</u>	Manual (On-line) Seismometer Status	6
	24 bits per subarray, as for Field 4.	
<u>Bytes 54-60</u>	Multisample Subarray Indicators	7
	8 bits (=1 byte) per subarray, according to the following code:	
	Bit on:	
	0 line decommissioned	
	1 subarray in total ICW scan	
	2 " being synchronized	
	3 " phone line being tested	
	4-7 spare	
	7 subarrays use 7 bytes.	
<u>Byte 61</u>	Padding byte, contains x'AA'	
<u>Byte 62-323</u>	1st Logical Record	
<u>Byte 324-585</u>	2nd Logical Record	
<u>Byte 586-847</u>	3rd Logical Record	

Byte 848-1109 4th Logical Record

Byte 1110-1371 5th Logical Record

Each logical record constitutes 262 bytes, and consists of a Status Field of 10 bytes and 7 pairs of Subarray Data Blocks (SDBs), one pair for each subarray, one SDB for each sample period (each subarray is sampled twice per decisecond). The formats of the Status Field and of an SDB are given below. See also Figure 1.

The format of the Status Field is as follows:

<u>Bytes</u>	<u>Contents</u>								
0	Length of this status field in bytes. (currently, 10)								
1	Version number of this status field. (Currently, 1)								
2-3	High rate sensor subjected to dc offset thresholding as follows: <table><thead><tr><th><u>Bit</u></th><th><u>Description</u></th></tr></thead><tbody><tr><td>0-1</td><td>Reserved (zero)</td></tr><tr><td>2</td><td>Set when sensor failed threshold</td></tr><tr><td>3-15</td><td>Sensor number</td></tr></tbody></table>	<u>Bit</u>	<u>Description</u>	0-1	Reserved (zero)	2	Set when sensor failed threshold	3-15	Sensor number
<u>Bit</u>	<u>Description</u>								
0-1	Reserved (zero)								
2	Set when sensor failed threshold								
3-15	Sensor number								
4-5	Low rate sensor, otherwise the same as bytes 2-3								
6-8	Discrete output fields transmitted as follows: <table><thead><tr><th><u>Bit</u></th><th><u>Description</u></th></tr></thead><tbody><tr><td>0-7</td><td>Subarray number to which transmitted</td></tr><tr><td>8-15</td><td>DOF1</td></tr><tr><td>16-23</td><td>DOF2</td></tr></tbody></table>	<u>Bit</u>	<u>Description</u>	0-7	Subarray number to which transmitted	8-15	DOF1	16-23	DOF2
<u>Bit</u>	<u>Description</u>								
0-7	Subarray number to which transmitted								
8-15	DOF1								
16-23	DOF2								
9	Spare (zero)								

Any fields lacking entries shall be coded zeros.

Each Subarray Data Block (SDB) contains data for one sample period from one subarray. Two consecutive SDBs are from one and the same subarray.

The SDB format is as follows:

<u>Field</u>	<u>Bytes</u>	<u>Contents</u>
1	0-3	Sample period indicators, according to the following layout:
	<u>Byte</u>	<u>Bit</u>
	0	0
		1
		2
		3
		4-7
	1	0
		1
		2
		3
		4-7
	2	0-3
		4-7
	3	0-5
		6-7

\* No data present in fields 2 and 3. They contain a direct transcription of the received message, including polynomial residual with the received sync pattern in field 2, and the rest of the message in field 3, with unused bytes set to zeros. Bits 0, 1 of Byte 0, all of Bytes 2-3 are zero.

<u>Field</u>	<u>Bytes</u>	<u>Contents</u>
2	4-5	<u>Submultiplex</u> channel data value, defloated with extended sign, right-justified in bits 0-13. Bits 14 and 15 are zero.
3	6-17	6 <u>sequential</u> channel values, in the same format as for Field 2.

As indicated under the description of Field 1, the SDB format is different when an ODW polynomial code error occurs.

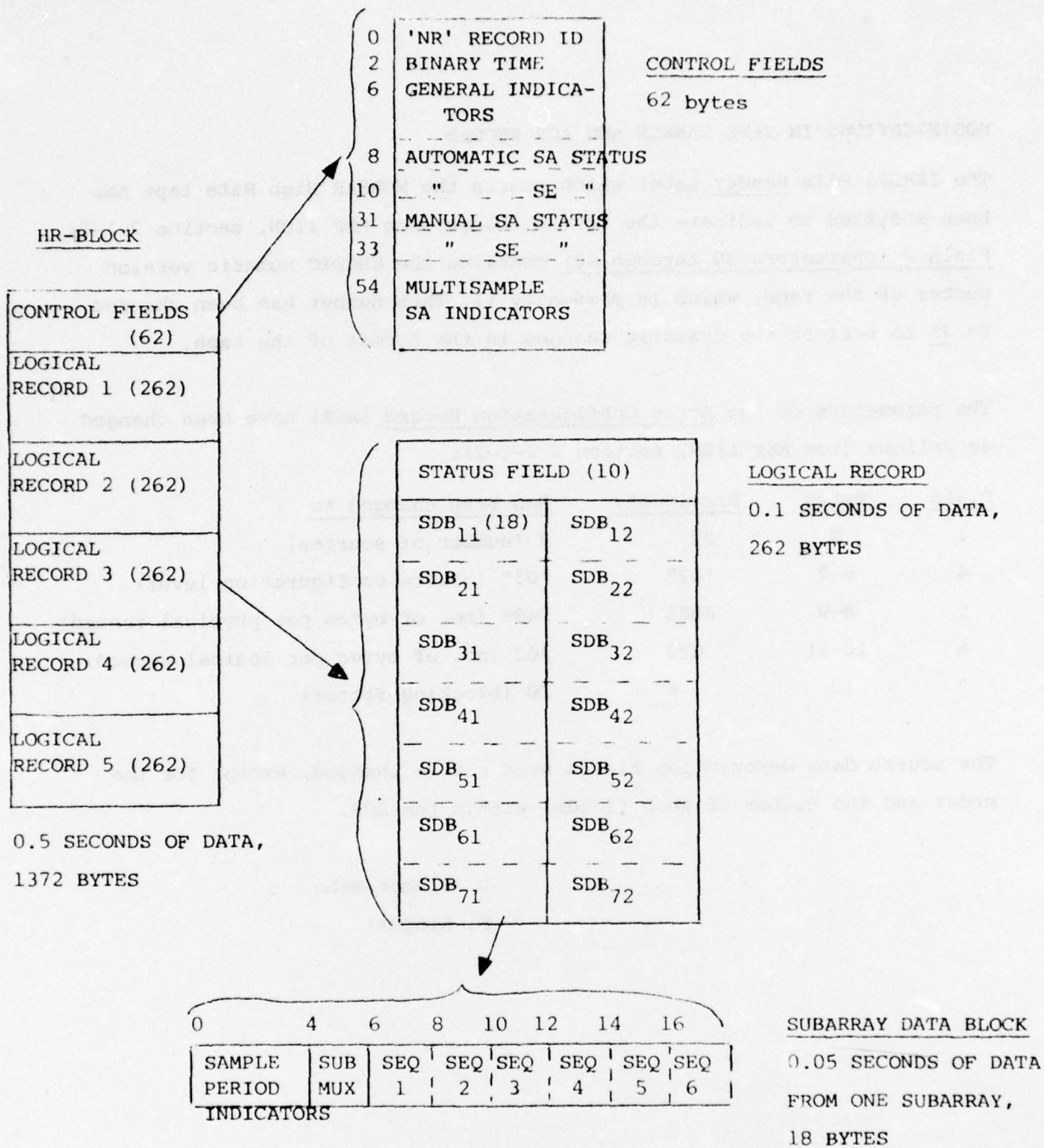


Figure 1: High Rate Block Layout. If 4 HR-blocks comprise 1 physical record on tape, then one tape may contain 3.97 hours of data.

3. MODIFICATIONS IN TAPE LABELS AND ACR RECORD

The ISRSPS File Header Label which starts the NORSAR High Rate tape has been modified to indicate the format change (see REF 110N, section 2-1-2). Field 7 (characters 39 through 40) contains the EBCDIC numeric version number of the tape, which is presently 11. This number has been changed to 21 to reflect the dramatic changes in the format of the tape.

The parameters of the Array Configuration Record (ACR) have been changed as follows (see REF 110N, section 2-2-1-2):

<u>Field</u>	<u>Bytes</u>	<u>Previously</u>	<u>Has been changed to</u>
1	2	22	7 (number of sources)
4	6-7	"02"	"03" (source configuration level)
5	8-9	4986	5488 (no. of bytes per physical record)
6	10-11	890	262 (no. of bytes per logical record)
7	12	5	20 (blocking factor)

The source data description fields need not be changed, except for the order and the number of such fields, within the ACR.

D. Rieber-Mohn

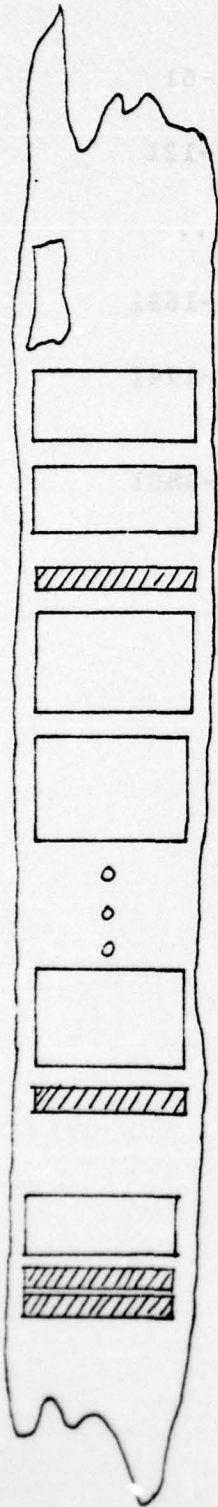
F. Ringdal

APPENDIX B

FORMAT OF NORSAR LOW RATE DATA TAPE EFFECTIVE 1 OCTOBER 1976

TAPE FORMAT - NORSAR LOW RATE TAPE

(Modified October 1976)



LOAD POINT

VOL-SERIAL HEADER RECORD (80 BYTES)

HEADER LABEL (80 BYTES)

END OF FILE (TAPE MARK)

DATA RECORD (1802 BYTES) (NR)

DATA RECORD (1802 BYTES) (NR)

•  
•  
TRANSATLANTIC DATA RECORD (XN)

•  
•  
DATA RECORD (1802 BYTES) (NR)

END OF FILE (TAPE MARK)

TRAILER LABEL (80 BYTES)

END OF FILE (TAPE MARK)

END OF FILE (TAPE MARK)

The tape contains records of types 'NR' and 'XN' in unpredictable order.



DATA RECORD FORMAT

'NR'	BYTES	0-1
DATA FRAME no 1	BYTES	2-61
DATA FRAME no 2	BYTES	62-121
	BYTES	....
DATA FRAME no 28	BYTES	1622-1681
DATA FRAME no 29	BYTES	1682-1741
DATA FRAME no 30	BYTES	1742-1801

TOTAL RECORD LENGTH = 1802 BYTES

FRAME LENGTH = 60 BYTES

VOL-SERIAL HEADER

BYTES	0-3	HEADER IDENTIFIER	'VOL1'
BYTES	4-9	VOL-SERIAL	e.g. '000013'
BYTE	10	SECURITY INDICATOR	'1'
BYTES	11-79	RESERVED FOR EXPANSION	'b...b'

TOTAL LENGTH IS 80 BYTES

NOTE: All data in this record should be interpreted as alphanumeric. 'VOL1' and '1' are fixed. The '1' actually implies a permanent retention cycle. The VOL-SERIAL represents the tape number.

HEADER LABEL

BYTES	0-3	IDENTIFIER	'HDR1'
BYTES	4-14	TAPE TYPE	'LOWbRATEbbb'
BYTES	15-20	LOCATION	'NDPCbb'
BYTES	21-26	VOL-SERIAL (THIS TAPE)	e.g. '000056'
BYTES	27-28	RESERVED	'bb'
BYTES	29-34	VOL-SERIAL (PREVIOUS TAPE)	e.g. '000055'
BYTES	35-36	LOCATION CODE	'03' (NDPC)
BYTES	37-38	TAPE TYPE CODE	'14' (LOW RATE)
BYTES	39-40	TAPE FORMAT VERSION	'02'
BYTES	41-46	DATE = 'BYRDAY'	e.g. 'b7Q181'
BYTES	47-52	RECYCLE DATE	'b99365'..
BYTE	53	RETENTION CODE	'1' (PERMANENT)
BYTES	54-59	DATE = 'BYRDAY'	SAME AS BYTES 41-46
BYTES	60-65	PROCESSING SYSTEM	'ISRSPS'
BYTES	66-79	COMMENTS	'NORSARbLPbDATA'

TOTAL LENGTH IS 80 BYTES

NOTE: All data in this record should be interpreted as alphanumeric characters.

TRAILER LABEL

BYTES	0-3	IDENTIFIER	'EOF1'
BYTES	4-28	RESERVED	'bb...bb'
BYTES	29-34	VOL-SERIAL (NEXT TAPE)	e.g. '000057'
BYTES	35-79	RESERVED	'bb....bb'

DATA FRAME FORMAT

LENGTH

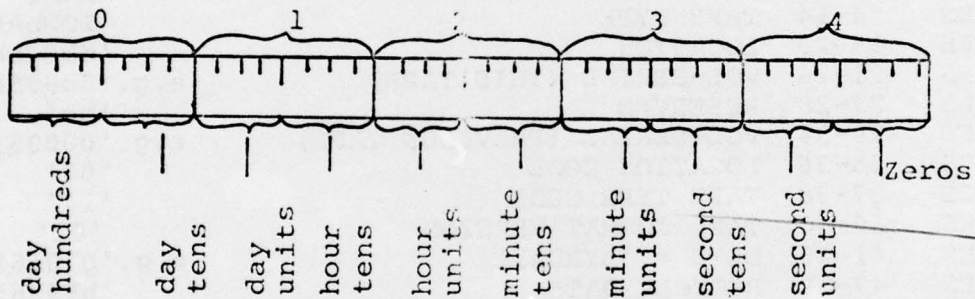
POSITION

5 BYTES	RAW TIMING WORD	0-4
1 BYTE	RAW SITE ERROR TABLE	5
4 BYTES	RAW SEIS FUNCTION TABLE	6-9
42 BYTES	RAW LONG PERIOD DATA	10-51
8 BYTES	FRAME FLAG BYTES	52-59

TOTAL LENGTH IS 60 BYTES

RAW TIMING WORD (5 BYTES 0-4)

FRAME  
BYTE



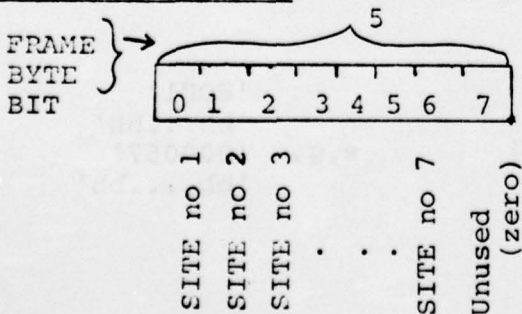
NOTE: Digits in timing word are single HEX digit-BCD

e.g.  $0010_2 = 2_{10} = 2_{16}$

$1001_2 = 9_{10} = 9_{16}$

HEX characters A thru F are illegal

RAW SITE ERROR TABLE (1 BYTE, 5)



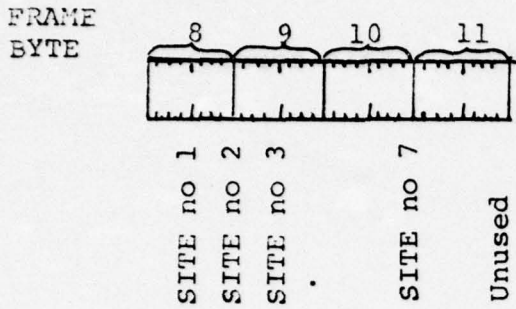
NOTE: One bit represents one site.

Bit Value = 0 : normal

Bit Value = 1 : abnormal

This bit configuration is to be referred to as the SIT format

RAW SEISMOMETER FUNCTION TABLE (4 BYTES 6-9)



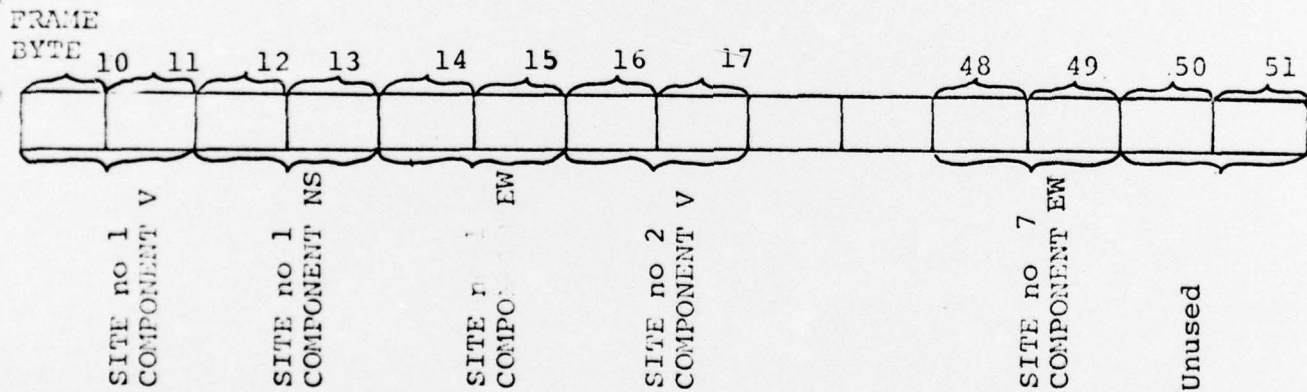
NOTE: Four bits represent one site-2 sites are represented in one byte.

Bit 0 or 4 corresponds to the Vertical component (V)  
 Bit 1 or 5 corresponds to the North-South component (NS)  
 Bit 2 or 6 corresponds to the East-West component (EW)  
 Bit 3 or 7 unused

Bit Value = 0 : normal site/component  
 Bit Value = 1 : abnormal site/component

NOTE: This configuration of bits will be denoted SFT format.

RAW LONG PERIOD DATA (42 BYTES 10-51)



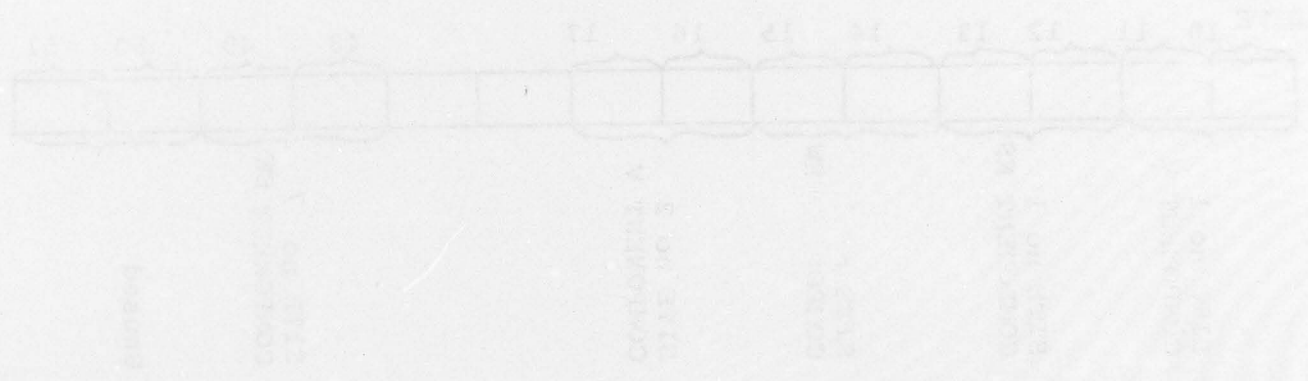
NOTE: Long Period Data is recorded on tape as integer halfwords. There are two bytes per sample point. The LP Data contains 7 sites with three components per site (the components vary most rapidly).

The Long Period Data values differs from those recorded on the NDPC data tapes by not having the low order two bits used for error checking. Thus before recording on the Low Rate tape takes place the data values received from SPS are divided by 4.

FRAME FLAG BYTES

(8 BYTES 52-59)

These eight bytes are unused and will always contain zeros.



NOTE: This configuration of bits will be used in the status frame format.

Bit Value = 1: Normal  
Bit Value = 0: Abnormal

NOTE: Four bits represent the data type as represented in one byte.

Bit 1 or 2 corresponds to the data type component (DT)  
Bit 3 or 4 corresponds to the data type component (DT)  
Bit 5 or 6 corresponds to the data type component (DT)  
Bit 7 or 8 corresponds to the data type component (DT)

APPENDIX C

NORSAR ARRAY BEAM DEPLOYMENT EFFECTIVE 1 OCTOBER 1976

NORSAR beam set valid from 1 October 1976. The first part of the table is the coherent beam set (beam set 451, 180 beams), while the second part is the incoherent beams (beam set 271, 64 beams). UX,UY given in the table corresponds to the slowness-space location where the phase given (PHASE) is expected to be observed for an event taking place at the latitude (LAT) and the longitude (LON) listed. Region number and name correspond to the Flinn and Engdahl (1965) regionalization.

H. Bungum  
F. Ringdal

References

Flinn, E.A., and E.R. Engdahl (1965): A proposed basis for geographical and seismic regionalization, Rev. Geophys., 3, 123-149.

NORSAR ARRAY BLAM SET 451 OCTOBER 1, 1976

BEAM NO	UX (S/KM)	UY (S/KM)	PHASE	LAT	LONG	REGION NUMBER AND NAME
1	0.0089900	-0.091390	P	63N	7W	641 NORTH OF SVALBARD
2	-0.0638110	-0.0873700	P	73N	55E	648 NOVAYA ZEMLYA
3	0.0443600	-0.0689300	P	72N	74W	642 HAFIN ISLAND REGION
4	0.0172400	-0.0659800	P	67N	137W	677 N. YUKON TERR., CANADA
5	0.0097600	-0.0690000	P	63N	151W	1 CENTRAL ALASKA
6	-0.0117700	-0.0648100	P	61N	148W	2 SOUTHERN ALASKA
7	0.0005800	-0.0645199	P	65N	165W	676 ALASKA
8	0.0184800	-0.0599800	P	59N	137W	19 SOUTHEASTERN ALASKA
9	0.0133000	-0.0617500	P	60N	146W	2 SOUTHERN ALASKA
10	0.0054900	-0.0602300	P	57N	158W	12 ALASKA PENINSULA
11	0.0093000	-0.0596800	P	57N	152W	13 KODIAK ISLAND REGION
12	0.0019500	-0.0575700	P	54N	163W	1 UNIMAK ISLAND REGION
13	-0.0317300	-0.0581200	P	62N	143E	671 EASTERN SIBERIA
14	-0.0038300	-0.0565900	P	52N	171W	9 FOX ISLANDS, ALEUTIANS
15	-0.0084800	-0.0557100	P	52N	178W	7 ANDREANOF IS., ALEUTIANS
16	-0.0118300	-0.0549600	P	52N	177E	6 RAT ISLANDS, ALEUTIANS
17	-0.0184400	-0.0554300	P	55N	166E	4 KOMANDORSKY ISLANDS REG.
18	-0.025266	-0.0558723	P	56N	162E	218 NEAR EAST COAST KAMCHATKA
19	0.0247000	-0.0545300	P	56N	131W	25 VANCOUVER ISLAND REGION
20	-0.0168600	-0.0545200	P	53N	169E	4 KOMANDORSKY ISLANDS REG.
21	-0.0219929	-0.0533326	P	52N	160E	219 OFF EAST COAST KAMCHATKA
22	0.0254800	-0.0511500	P	44N	129W	3 OFF COAST OF OREGON
23	-0.0263916	-0.0507930	P	50N	155E	221 KURILE ISLANDS
24	-0.0699700	-0.0529800	P	67N	67E	335 URAL MOUNTAINS REGION
25	0.0372900	-0.0486100	P	42N	112W	457 EASTERN IDAHO
26	-0.0282200	-0.0488500	P	47N	154E	221 KURILE ISLANDS
27	0.0342800	-0.0461600	P	37N	116W	41 SOUTHERN NEVADA
28	0.0296800	-0.0454700	P	37N	122W	39 CENTRAL CALIFORNIA
29	-0.0322567	-0.0457137	P	44N	150E	222 KURILE ISLANDS REGION
30	0.0423000	-0.0440100	P	40N	105W	479 COLORADO
31	-0.0366555	-0.0431740	P	43N	144E	274 HOKKAIDO, JAPAN, REGION
32	-0.0567600	-0.0429400	P	56N	111E	327 LAKE BAIKAL REGION
33	0.0322590	-0.0406344	P	32N	117W	45 CALIFORNIA-MEXICO BORDER
34	-0.0381218	-0.0406344	P	41N	142E	224 HOKKAIDO, JAPAN, REGION
35	0.0337253	-0.0380947	P	29N	114W	48 BAJA CALIFORNIA
36	-0.0395880	-0.0380947	P	39N	140E	227 HONSHU, JAPAN
37	-0.0381218	-0.0355551	P	34N	142E	229 OFF E COAST HONSHU, JAPAN
38	-0.0410543	-0.0355551	P	36N	138E	227 HONSHU, JAPAN
39	0.0523500	-0.0326000	P	37N	90W	485 EASTERN MISSOURI
40	0.0360600	-0.0341800	P	25N	110W	49 GULF OF CALIFORNIA
41	-0.0379400	-0.0338000	P	31N	142E	211 SOUTH OF HONSHU, JAPAN
42	-0.0425206	-0.0330154	P	34N	135E	233 NEAR S COAST OF S. HONSHU
43	-0.0339000	-0.0294900	P	18N	146E	216 MARIANA ISLANDS
44	-0.0394700	-0.0315200	P	29N	139E	211 SOUTH OF HONSHU, JAPAN
45	-0.0439500	-0.0309300	P	32N	132E	236 SHIKOKU, JAPAN
46	0.0343600	-0.0283100	P	19N	109W	53 REVILLA GIGEDO ISLANDS
47	-0.0456800	-0.0269000	P	27N	129E	238 RYUKYU ISLANDS
48	-0.0547600	-0.0272300	P	37N	115E	658 NORTHEASTERN CHINA
49	-0.0895300	-0.0272300	P	61N	56E	335 URAL MOUNTAINS REGION
50	0.0381241	-0.0253965	P	19N	102E	57 MICHACAN, MEXICO
51	-0.0470900	-0.0254200	P	26N	126E	238 RYUKYU ISLANDS
52	0.0429200	-0.0219900	P	17N	96W	61 OAXACA, MEXICO
53	-0.0493600	-0.0217700	P	23N	121E	244 TAIWAN
54	0.0915100	-0.0193800	P	58N	33W	402 NORTH ATLANTIC OCEAN
55	0.0354900	-0.0207200	P	9N	103W	63 OFF COAST OF MEXICO
56	0.0425229	-0.0177776	P	14N	92W	64 NEAR COAST OF CHIAPAS, MEX
57	-0.0450100	-0.0184400	P	11N	125E	251 SAMAR, PHILIPPINE ISLANDS
58	-0.0472800	-0.0183900	P	16N	121E	249 LUZON, PHILIPPINE ISLANDS
59	-0.0710800	-0.0166000	P	50N	79E	329 EASTERN KAZAKH SSR
60	0.0477700	-0.0162600	P	17N	87W	94 CARIBBEAN SEA
61	-0.0586495	-0.0152379	P	27N	105E	664 EASTERN CHINA
62	-0.0615821	-0.0152379	P	33N	99E	325 TSINGHAI PROVINCE, CHINA
63	-0.0674471	-0.0152379	P	43N	89E	332 NORTHERN SINKIANG PROV.
64	0.0452500	-0.0135000	P	12N	87W	74 NEAR COAST OF NICARAGUA
65	-0.0659809	-0.0126983	P	38N	91E	325 TSINGHAI PROVINCE, CHINA
66	0.0373800	-0.0098600	P	0N	91W	697 GALAPAGOS ISLANDS
67	-0.0453500	-0.0108600	P	0N	121E	265 NORTHERN GLEBELS
68	-0.0586495	-0.0101586	P	23N	101E	318 YUNAN PROVINCE, CHINA
69	-0.0615821	-0.0101586	P	28N	96E	313 INDIA-CHINA BORDER REGION
70	-0.0645146	-0.0101586	P	33N	92E	325 TSINGHAI PROVINCE, CHINA
71	-0.0674471	-0.0101586	P	38N	87E	321 SOUTHERN SINKIANG PROV.
72	0.0443300	-0.0077000	P	8N	92W	80 PANAMA-COSTA RICA BORDER
73	0.0396500	-0.0067200	P	3N	84W	76 OFF COAST OF CENT. AMERICA
74	-0.0659809	-0.0076190	P	33N	89E	306 TIBET
75	0.0566300	-0.0043200	P	20N	71W	88 DOMINICAN REPUBLIC REGION
76	0.0458900	-0.0043500	P	8N	78W	81 PANAMA
77	-0.0615821	-0.0050793	P	23N	94E	294 BURMA-INDIA BORDER REGION
78	-0.0645146	-0.0050793	P	28N	90E	306 TIBET
79	-0.0714999	-0.0063000	P	41N	79E	321 KIRGIZ-SINKIANG BORDER
80	-0.061158	-0.0025397	P	17N	94E	296 BURMA
81	-0.0689133	-0.0025397	P	34N	83E	306 TIBET
82	0.0370100	0.0004700	P	7S	80W	178 OFF COAST OF N. PERU
83	-0.0512500	0.0005400	P	2N	98E	706 NORTHERN SUMATRA
84	-0.0586495	0.0	P	12N	93E	703 ANDAMAN ISLANDS REGION
85	0.0578500	0.0020200	P	19N	65W	70 PUERTO RICO REGION
86	0.0496600	0.0020000	P	10N	71W	10 LAKE MARACAIBO
87	-0.0700300	0.0027200	P	32N	79E	314 KASHMIR-TIBET BORDER REG.
88	-0.0718459	0.0025396	P	35N	77E	332 EASTERN KASHMIR
89	-0.0747785	0.0025396	P	41N	72E	716 KIRGIZ SSR
90	-0.0839100	0.0024000	P	52N	55E	335 URAL MOUNTAINS REGION

PRECEDING PAGE BLANK-NOT FILMED

BEAM NO	UX (S/KM)	UY (S/KM)	PHASE	LAT	LOX	REGION NUMBER AND NAME
91	0.0855800	0.0076700	P	51N	30W	433 NORTH ATLANTIC RIDGE
92	0.0572300	0.0080400	P	16N	61W	92 LEIWARD ISLANDS
93	-0.0718459	0.0076189	P	32N	74E	711 SOUTHWESTERN KASHMIR
94	-0.0747785	0.0076189	P	37N	71E	717 AFGHANISTAN-USSR BORDER
95	0.0533820	0.0090000	P	11N	62W	95 WINDWARD ISLANDS
96	0.0365430	0.0116300	P	10S	71W	112 PERU-BRAZIL BORDER REGION
97	-0.0760000	0.0127000	P	36N	67E	718 HINDU KUSH REGION
98	-0.0654000	0.0157700	P	17N	74E	314 INDIA
99	-0.0725600	0.0149800	P	30N	69E	71 PAKISTAN
100	0.0333500	0.0175700	P	18S	64W	12 BOLIVIA
101	0.0674494	0.0203172	P	28N	45W	473 NORTH ATLANTIC RIDGE
102	-0.0718300	0.0193300	P	27N	67E	71 PAKISTAN
103	-0.0863900	0.0210700	P	48N	48E	336 WESTERN KAZAKH SSR
104	0.0574800	0.0232100	P	18N	47W	433 NORTH ATLANTIC RIDGE
105	-0.0772099	0.0232200	P	35N	59E	348 IRAN
106	0.0761000	0.0282800	P	41N	30W	434 AZORES ISLANDS REGION
107	0.0508500	0.0288400	P	12N	45W	473 NORTH ATLANTIC RIDGE
108	-0.0434500	0.0274300	P	14S	66E	427 MID-INGIAN RISE
109	-0.0546200	0.0271900	P	1N	66E	421 CARLSBERG RIDGE
110	-0.0724300	0.0270400	P	27N	60E	353 SOUTHERN IRAN
111	-0.0725000	0.0324000	P	28N	59E	353 SOUTHERN IRAN
112	-0.0773000	0.0335000	P	36N	50E	346 IRAN
113	-0.0807800	0.0329800	P	43N	45E	337 EASTERN CAUCASUS
114	-0.0589800	0.0350300	P	10N	57E	421 CARLSBERG RIDGE
115	-0.0622200	0.0349200	P	15N	56E	417 ARABIAN SEA
116	-0.0732000	0.0364000	P	31N	50E	348 IRAN
117	-0.0732000	0.0406000	P	34N	46E	347 WESTERN IRAN
118	0.0659500	0.0419000	P	37N	25W	435 AZORES ISLANDS
119	0.0414900	0.0439400	P	4N	33W	436 C. MID-ATLANTIC RIDGE
120	-0.0577300	0.0428700	P	13N	49E	485 EASTERN GULF OF ADEN
121	-0.0736000	0.0429700	P	39N	41E	366 TURKEY
122	0.0110600	0.0455900	P	23S	13W	417 SOUTH ATLANTIC RIDGE
123	-0.0188100	0.0454100	P	26S	28E	584 REPUBLIC OF SOUTH AFRICA
124	0.0325800	0.0493900	P	1N	26W	426 C. MID-ATLANTIC RIDGE
125	-0.0222700	0.0506600	P	17S	29E	58 RHODESIA
126	-0.0293800	0.0508200	P	11S	34E	577 MALAWI
127	-0.0459100	0.0538200	P	10N	39E	558 ETHIOPIA
128	0.0258300	0.0550400	P	0N	18W	406 C. MID-ATLANTIC RIDGE
129	0.0185000	0.0547000	P	7S	13W	458 ASCENSION ISLAND REGION
130	-0.0528700	0.0555800	P	20N	39E	555 WESTERN ARABIAN PENINSULA
131	-0.0298600	0.0596300	P	1N	30E	568 UGANDA
132	-0.0687600	0.0597700	P	41N	33E	366 TURKEY
133	-0.0811900	0.0575800	P	45N	34E	361 CRIMEA REGION
134	-0.0581000	0.0616500	P	35N	33E	372 CYPRUS
135	0.0441000	0.0659200	P	36N	11W	402 NORTH ATLANTIC OCEAN
136	-0.0561400	0.0702200	P	39N	28E	366 TURKEY
137	-0.0381218	0.0761895	P	35N	24E	370 CRETE
138	0.0110300	0.0846300	P	36N	5E	396 ALGERIA
139	-0.0082600	0.1054600	P	44N	12E	545 NORTHERN ITALY
140	-0.0166900	0.0918900	P	39N	15E	39 SOUTHERN ITALY
141	-0.0295100	0.1043299	P	43N	17E	383 YUGOSLAVIA
142	-0.0337230	0.0787292	P	36N	22E	168 SOUTHERN GREECE
143	-0.0440400	0.0806600	P	39N	24E	365 AEGEAN SEA
144	-0.0731699	0.0846900	P	46N	27E	350 ROMANIA
145	-0.0540100	-0.0474300	PP	14N	145E	216 MARIANA ISLANDS
146	-0.0433800	-0.0457300	PP	9S	159E	193 SOLOMON ISLANDS
147	-0.0493300	-0.0420300	PP	5S	152E	192 NEW BRITAIN REGION
148	-0.0677900	-0.0285600	PP	20N	121E	248 PHILIPPINE ISLANDS REGION
149	-0.0615821	-0.0253965	PP	2S	132E	196 WEST NEW GUINEA REGION
150	-0.0653400	-0.0242600	PP	5N	126E	254 MINDANAO, PHILIPPINE IS.
151	-0.0684900	-0.0244300	PP	13N	121E	25 MINDORO, PHILIPPINE IS.
152	-0.0111900	-0.0285900	PKP	24S	176W	171 SOUTH OF FIJI ISLANDS
153	-0.0136800	-0.0286900	PKP	25S	180W	171 SOUTH OF FIJI ISLANDS
154	-0.0135100	-0.0225700	PKP	32S	179W	179 SOUTH OF KERMADEC ISLANDS
155	-0.0170200	-0.0165400	PKP	14S	167E	186 NEW HEBRIDES ISLANDS
156	-0.0081300	-0.0153900	PKP	16S	174W	173 TONGA ISLANDS
157	-0.0114500	-0.0154600	PKP	19S	179W	181 FIJI ISLANDS REGION
158	-0.0153400	-0.0160500	PKP	23S	172E	149 LOYALTY ISLANDS REGION
159	-0.0189700	-0.0139700	PKP	8S	158E	193 SOLOMON ISLANDS
160	-0.0201300	-0.0122100	PKP	5S	152E	192 NEW BRITAIN REGION
161	-0.0241300	-0.0064500	PKP	9S	130E	29 TIMOR SEA
162	0.0112900	-0.0030500	PKP	23S	113W	683 EASTERN ISLAND REGION
163	0.0116700	0.0022500	PKP	36S	103W	692 SOUTHERN PACIFIC OCEAN
164	0.0108500	0.0027400	PKP	42S	90W	692 SOUTHERN PACIFIC OCEAN
165	0.0115400	0.0095400	PKP	30S	71W	135 NEAR COAST OF S. CHILE
166	0.0090200	0.0114700	PKP	46S	75W	144 NEAR COAST OF S. CHILE
167	-0.0013500	0.0203000	PKP	59S	26W	153 SOUTH SANDWICH IS. REGION
168	-0.0052000	0.0219000	PKP	55S	2W	41 SOUTH ATLANTIC RIDGE
169	-0.0106000	0.0205700	PKP	54S	27E	433 SOUTH OF AFRICA
170	-0.0330600	-0.0060300	PKKP	16S	73W	115 NEAR COAST OF PERU
171	0.0216200	0.0132000	PKKP	6S	131E	281 TANIMBAR ISLANDS REGION
172	0.0180800	0.0116800	PKKP	11N	121E	254 PANAY, PHILIPPINE ISLANDS
173	0.0183900	0.0196500	PKKP	4S	142E	22 NEW GUINEA
174	0.0187900	0.0238300	PKKP	7S	148E	277 EAST NEW GUINEA REGION
175	0.0159600	0.0278000	PKKP	7S	154E	193 SOLOMON ISLANDS
176	-0.0097400	-0.0391300	SKP	19S	175W	173 TONGA ISLANDS
177	-0.0134400	-0.0381900	SKP	19S	179W	181 FIJI ISLANDS REGION
178	-0.0258400	-0.0332200	SKP	18S	168E	186 NEW HEBRIDES ISLANDS
179	-0.0057900	-0.0359900	PCP	52N	174W	7 ALUTKA IS.
180	-0.0192600	-0.0339000	PCP	51N	158E	214 NEAR EAST COAST KAMCHATKA

NORSAR ARRAY BEAM SET 271 OCTOBER 1, 1976

BLAM NO	UX (S/KM)	UY (S/KM)	PHASE	LAT	LOX	REGION NUMBER AND NAME
1	0.0089900	-0.0913300	P	43N	7W	641 NORTH OF SVALBARD
2	-0.0638100	-0.0873700	P	73N	55E	648 NOUVAYA ZEMLYA
3	0.0194000	-0.0634400	P	61N	152W	2 SOUTH IN ALASKA
4	0.0019500	-0.0575700	P	54N	163W	1 UNIMAK ISLAND REGION
5	-0.0084800	-0.0557100	P	52N	178W	7 ADIRLAK OF IS., ALEUTIANS
6	-0.0205266	-0.0558723	P	56N	162E	218 NEAR EAST COAST KAMCHATKA
7	0.0247000	-0.0545300	P	50N	130W	25 VANCOUVER ISLAND REGION
8	-0.0151900	-0.0542300	P	52N	172E	5 NEAR ISLANDS, ALEUTIAN
9	0.0382900	-0.0498000	P	44N	111W	458 HERGEN LAKE REGION
10	-0.0699700	-0.0509800	P	67N	67E	315 URAL MOUNTAINS REGION
11	-0.0282200	-0.0488500	P	47N	154E	221 KURILL ISLANDS
12	-0.0366555	-0.0431740	P	43N	144E	224 HOKKAIDO, JAPAN, REGION
13	-0.0567600	-0.0424400	P	56N	111E	327 LAKE BAIKAL REGION
14	0.0347900	-0.0412400	P	31N	114W	49 GULF OF CALIFORNIA
15	-0.0379400	-0.0338000	P	31N	142E	211 SOUTH OF HONSHU, JAPAN
16	-0.0339000	-0.0294900	P	18N	146E	216 MARIANA ISLANDS
17	0.0343600	-0.0281100	P	19N	109W	53 REVILLA GIGEDO ISLANDS
18	-0.0456800	-0.0269000	P	27N	129E	238 RYUKYU ISLANDS
19	-0.0547600	-0.0272300	P	37N	115E	658 NORTHEASTERN CHINA
20	-0.0895300	-0.0272300	P	61N	56E	335 URAL MOUNTAINS REGION
21	-0.0493600	-0.0217700	P	23N	121E	244 TAIWAN
22	-0.0729899	-0.0238100	P	54N	81E	326 CENTRAL RUSSIA
23	0.0915100	-0.0193800	P	58N	33W	42 NORTH ATLANTIC OCEAN
24	0.0425229	-0.0177776	P	14N	92W	69 NEAR COAST OF CHIAPAS, MEX
25	-0.0442800	-0.0163500	P	5N	126E	259 MINDANAO, PHILIPPINE IS.
26	-0.0636700	-0.0155100	P	37N	96E	325 TSINGHAI PROVINCE, CHINA
27	-0.0689133	-0.0126983	P	42N	86E	337 NORTHERN SINKIANG PROV
28	-0.1005400	-0.0126800	P	58N	50E	724 WESTERN RUSSIA
29	-0.0615821	-0.0050793	P	23N	94E	294 BURMA-INDIA BORDER REGION
30	-0.0718459	-0.0025397	P	39N	78E	321 SOUTHERN SINKIANG PROV
31	-0.0478000	0.0	P	8S	105E	282 SOUTH OF JAVA
32	-0.0566000	0.0007900	P	9N	94E	704 NICOBAR ISLANDS REGION
33	0.0578500	0.0020200	P	19N	65W	90 PUERTO RICO REGION
34	-0.0685900	0.0024400	P	24N	81E	311 NEPAL
35	-0.0747785	0.0025396	P	41N	72E	716 KIRGIZ SSR
36	-0.0839100	0.0024000	P	52N	55E	335 URAL MOUNTAINS REGION
37	-0.1055599	0.00061700	P	55N	45E	724 WESTERN RUSSIA
38	-0.0747785	0.0076189	P	37N	71E	717 AFGHANISTAN-USSR BORDER
39	-0.0725600	0.0149800	P	30N	69E	71 PAKISTAN
40	-0.1031500	0.0158000	P	53N	44E	724 WESTERN RUSSIA
41	-0.0803900	0.0210700	P	48N	48E	336 WESTERN KAZAKH SSR
42	0.0796000	0.0227600	P	46N	28W	423 NORTH ATLANTIC RIDGE
43	-0.0772099	0.0232200	P	35N	59E	348 IRAN
44	0.0733145	0.0253965	P	36N	36W	404 NORTH ATLANTIC RIDGE
45	-0.0500800	0.0265900	P	5S	68E	476 CHAGOS ARCHIPELAGO REGION
46	0.0483880	0.0330154	P	11N	42W	403 NORTH ATLANTIC RIDGE
47	-0.0725000	0.0324000	P	28N	55E	353 SOUTHERN IRAN
48	-0.0807800	0.0329800	P	43N	45E	337 EASTERN CAUCASUS
49	-0.0622200	0.0349200	P	15N	56E	417 ARABIAN SEA
50	-0.0732000	0.0406000	P	34N	46E	347 WESTERN IRAN
51	0.0132100	0.0485400	P	18S	13W	41 SOUTH ATLANTIC RIDGE
52	-0.0516000	0.0512000	P	12N	43E	555 WESTERN ARABIAN PENINSULA
53	0.0258335	0.0550400	P	0N	18W	476 G. MID-ATLANTIC RIDGE
54	-0.0270400	0.0562700	P	7S	30E	572 LAKE TANGANYIKA REGION
55	-0.0811900	0.0575800	P	45N	34E	361 CRIMEA REGION
56	0.0441000	0.0659200	P	36N	11W	472 NORTH ATLANTIC OCEAN
57	-0.0452900	0.0716799	P	35N	27E	369 JUBECANESE ISLANDS
58	-0.0561400	0.0702200	P	39N	28E	366 TURKEY
59	-0.0336800	0.0836400	P	38N	21E	364 GREECE
60	-0.0135100	-0.0225700	PKP	32S	179W	173 SOUTH OF KERMADEC ISLANDS
61	-0.0170200	-0.0165400	PKP	14S	167E	186 NEW HEBRIDES ISLANDS
62	-0.0084000	-0.0148100	PKP	20S	175W	173 TONGA ISLANDS
63	-0.0201300	-0.0122100	PKP	5S	152E	142 NEW BRITAIN REGION
64	-0.0013500	0.0200600	PKP	59S	26W	153 SOUTH SANDWICH IS. REGION